Khan, A., Percival, C., Caravan, R., Taatjes, C., & Shallcross, D. (2018). Criegee Intermediates and their impacts on the troposphere. *Environmental Science: Processes and Impacts*, *20*(3), 437-453. https://doi.org/10.1039/C7EM00585G

Peer reviewed version

Link to published version (if available):
10.1039/C7EM00585G

Link to publication record in Explore Bristol Research
PDF-document

University of Bristol - Explore Bristol Research
General rights

Environmental Science
Processes & Impacts

Accepted Manuscript

Volume 18 | Number 1 | January 2016 | Pages 1–152

Environmental Science
Processes & Impacts

rsc.li/process-impacts

ISSN 2050-7887

PAPER
Clare L. S. Wiseman et al
Geochemical behaviour of palladium in soils and Pd/PdO model
substances in the presence of the organic complexing agents
L-methionine and citric acid

175 YEARS
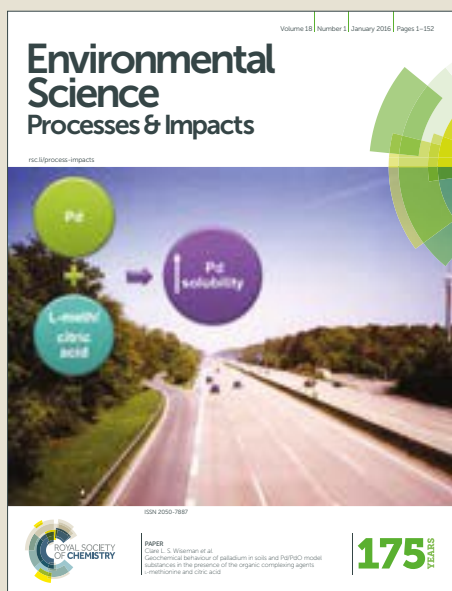
ROYAL SOCIETY
OF CHEMISTRY

rsc.li/process-impacts

Environmental Science: Processes & Impacts

ARTICLE

Criegee Intermediates and their impacts on the troposphere

M. A. H. Khan,[a] C. J. Percival,[b] R. L. Caravan,[c] C. A. Taatjes[c] and D. E. Shallcross[a, †]

Criegee intermediates (CIs), carbonyl oxides formed in ozonolysis of alkenes, play key roles in the troposphere. The decomposition of CIs can be a significant source of OH to the tropospheric oxidation cycle especially during nighttime and winter months. A variety of model-measurement studies have estimated surface-level stabilized Criegee intermediate (sCI) concentrations on the order of 1×10^4 cm^{-3} to 1×10^5 cm^{-3}, which makes a non-negligible contribution to the oxidising capacity in the terrestrial boundary layer. The reactions of sCI with the water monomer and the water dimer have been found to be the most important bimolecular reactions to the tropospheric sCI loss rate, at least for the smallest carbonyl oxides; the products from these reactions (e.g. hydroxymethyl hydroperoxide, HMHP) are also of importance to the atmospheric oxidation cycle. The sCI can oxidise SO_2 to form SO_3, which can go on to form a significant amount of H_2SO_4 which is a key atmospheric nucleation species and therefore vital to the formation of clouds. The sCI can also react with carboxylic acids, carbonyl compounds, alcohols, peroxy radicals and hydroperoxides, and the products of these reactions are likely to be highly oxygenated species, with low vapour pressures, that can lead to nucleation and SOA formation over terrestrial regions.

Environmental Significance

Criegee intermediates (CI) have been elusive moieties in the gas-phase until recently but have extremely interesting kinetic and mechanistic properties. The paper reviews the concentrations of stabilized CI on regional and global scales, the unimolecular decomposition of CI and bimolecular reactions of stabilized CI with a series of compounds. The potential role of the products of these reactions in atmospheric chemistry have been discussed which can alter our thinking about the oxidising capacity of the Earth's atmosphere and the rate of generation of secondary organic aerosol (SOA).

[a.] School of Chemistry, University of Bristol, Cantock's Close, Bristol BS8 1TS, UK.
[b.] Jet Propulsion Laboratory, California Institute of Technology, 4800 Oak Grove Dr, Pasadena, CA 91109, USA.
[c.] Combustion Research Facility, Mailstop 9055, Sandia National Laboratories, Livermore, California, 94551 USA.
† Author to whom correspondence should be sent
E-mail: d.e.shallcross@bristol.ac.uk, Phone: +44 (0) 117 928 7796

Formation of Criegee Intermediates

The ozonolysis of alkenes proceeds *via* carbonyl oxide intermediates; Rudolph Criegee first proposed this scheme in 1949 in the aqueous phase.[1] The reaction proceeds in two distinct steps; the first being a 1,3-cycloaddition of ozone across a double bond to form a primary ozonide, followed by decomposition to a carbonyl and a carbonyl oxide (Figure 1), otherwise known as a Criegee intermediate (CI).[2] This mechanism is also followed in the gaseous phase, and therefore in the atmosphere.
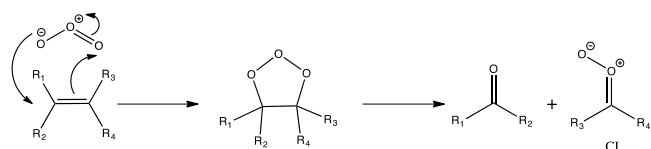

Figure 1. Formation of a primary ozonide followed by decomposition to a carbonyl and Criegee intermediate

The primary ozonide formed from the reaction of ozone with an alkene is very energy rich, and dissociates into a stable carbonyl compound and a vibrationally excited Criegee intermediate (CI*). The CI* can then either undergo unimolecular decomposition or can form a stabilised Criegee intermediate (sCI) *via* collisional relaxation.[3]

sCI can also be formed in the troposphere through radical-radical reactions (e.g. CH_3O_2 + BrO^4, CH_3O_2 + $+OH^5$ and CH_3O_2 + Cl^6), but their contribution to the total sCI is negligible.

Unimolecular decomposition of Criegee Intermediates and formation of OH

The reaction of the alkenes with ozone can be the major chemical sink of alkenes in heavily polluted areas,

depending on conditions. OH radicals can be produced from the ozonolysis of alkenes via either prompt formation from CI* or formation from the decomposition of sCIs at different species-dependent rates (Table 1). There has been an increasing amount of interest in CI chemistry in recent years after the realisation that the decomposition of the CI species can result in significant production of OH and HO_2 radicals which affects the oxidising capacity of the atmosphere.[7,8] Experimental measurement of OH radical yields from alkene ozonolysis through CI formation has historically proved to be difficult, because the OH radical formed quickly reacts with the original alkene or other decomposition products. In the past this has been circumvented by adding OH scavenger molecules (e.g. alkanes) to the reaction mixture, so that the rate of scavenger decay is indicative of OH concentration.[9] However, newer experimental methods employ direct measurement by laser-induced fluorescence (LIF) spectroscopy.[7,10-14] Production of the OH radical *via* the CI decomposition is thought to occur mainly through the *syn*-conformation.[15] This proceeds *via* isomerisation to a vinyl hydroperoxide, followed by the cleavage of the O-OH bond.[16-17] The OH production from the *anti*-conformation is also possible via isomerization of the molecule to a carboxylic acid followed by cleavage of the C-OH bond.[13,18]

Journal Name

ARTICLE

Table 1: The first order rate coefficients for the total sCI loss

Species	Rate coefficient (s^{-1})		Reaction conditions (Pressure, p and Temperature, T)	References
	Experimental	Theoretical		
CH$_2$OO		0.33	High p limit, T=298 K	Olzmann et al.[17]
		0.31	High p limit, T=298 K	Long et al.[19]
	0.19 ± 0.07^Y		p= 760 Torr, T=297 ± 1 K	Berndt et al.[20]
	0.23 ± 0.12^Y		p= 760 Torr, T=293 ± 0.5 K	Berndt et al.[20]
	11.6 ± 8.0$^\xi$		p= 7-30 Torr, T=293 K	Chhantyal-Pun et al.[21]
	96-246$^\xi$		p= 25 Torr N$_2$, T=297 K	Buras et al.[22]
	8-249$^\xi$		p= 50 Torr N$_2$, T=297 K	Buras et al.[22]
	73-283$^\xi$		p= 100 Torr N$_2$, T=297 K	Buras et al.[22]
	80-100^Y		p= 50-200 Torr, T=295 K	Liu et al.[23]
	115 ± 20$^\xi$		p= 5.1 Torr, T=295 K	Sheps[24]
	44.8 ± 11.9^Y		p= 760 Torr, T=297 K	Ouyang et al.[25]
CH$_3$CHOO		67.2(*anti*)	High p limit, T=298 K	Kuwata et al.[26]
		24.2(*syn*)	High p limit, T=298 K	Kuwata et al.[26]
		55.4(*anti*)	High p limit, T=298 K	Long et al.[19]
		328(*syn*)	High p limit, T=298 K	Long et al.[19]
		166(*syn*)	High p limit, T=298 K	Fang et al.[27]
	≤ 20^Y		p= 700 Torr, T=300 K	Herron et al.[28]
	288 ± 275(*syn*)^Y		p= 760 Torr, T=293-303 K	Newland et al.[29]
	3-30(*syn*)^Y		p= 735 Torr, T=293 K	Novelli et al.[30]
	≤250$^\xi$		p= 4 Torr, T=298 K	Taatjes et al.[31]
	2.9 ± 0.9^Y		p= 760 Torr, T=293 ± 0.5 K	Berndt et al.[32]
	76^Y		p= 760 Torr, T=298 K	Fenske et al.[33]
	2.5^Y		p= 758±4 Torr, T=297±3 K	Horie and Moortgat[3]
(CH$_3$)$_2$COO	6.4 ± 0.9^{Y,*}	3.5	p= 100 Torr	Kroll et al.[12]
	2.7 ± 0.7^{Y,*}	2.6	p= 10 Torr	Kroll et al.[12]
		250	High p limit, T=298 K	Olzmann et al.[17]
		369	High p limit, T=298 K	Fang et al.[27]
	305 ± 70$^\xi$		p= 10-100 Torr, T=293 K	Chhantyal-Pun et al.[34]
	361 ± 49$^{\xi,**}$		p= 200 Torr, T=298 K	Smith et al.[35]
	269 ± 82$^{\xi,**}$		p= 200 Torr, T=283 K	Smith et al.[35]
	916 ± 56$^{\xi,**}$		p= 200 Torr, T=323 K	Smith et al.[35]
	3.0 ± 0.4^Y		p= 760 Torr, T=293 ± 0.5 K	Berndt et al.[32]
	151 ± 35^Y		p= 760 Torr, T=298-299 K	Newland et al.[29]
Σ(MVKOO +MACROO)	26 ± 27^Y		p= 760 Torr, T=287-302 K	Newland et al.[29]
α-pinene sCI	<240± 44 (*syn*)^Y		p= 760 Torr, T=287-302 K	Newland et al.[36]
β-pinene sCI	<170± 38 (*syn*)^Y		p= 760 Torr, T=287-302 K	Newland et al.[36]
Limonene sCI	>130± 3 (*syn*)^Y		p= 760 Torr, T=287-302 K	Newland et al.[36]

Note: the experimental first order rate coefficients include a component from wall loss of the Criegee intermediate in addition to unimolecular decomposition, *the wall loss was negligible in the work of Kroll et al[9] because of using large diameter reactor, **the wall loss (assuming equal to thermal decomposition of CH$_2$OO) was accounted for in the work of Smith et al[35]. MVKOO represents methyl vinyl carbonyl oxide and MACROO represents methacrolein oxide which are isoprene derived sCIs. $^\xi$The values are from direct monitoring of the sCI decay, ^{Y}The values are from indirect sCI measurements.

Day-time OH radical production is dominated by the photolysis of ozone, but it has been widely documented in research that CI decomposition is one of the important sources of atmospheric OH.[27,30,37] The decomposition of CI can be a major source of night-time OH and up to ~24% of daytime OH production.[38] The PUMA campaign[37] (an intensive field study in Birmingham, UK) has also shown that CI decomposition is of large significance in OH winter concentrations. A 15-fold decrease in OH production should be expected in the winter months at higher latitudes compared with the summer months, due to low UV intensity retarding the ozone photolysis pathway, but only a 2-fold

decrease in OH concentration is seen due to the formation of OH through the efficient ozonolysis of alkenes.[37] Elshorbany et al.[39] also reported a significant daytime OH formation (24%) through ozone-alkene reactions in the urban area of Santiago, Chile. The ozonolysis of the alkenes increases with increasing temperature,[40] thus the largest production of OH through the formation of CIs is expected over tropical regions and alkene-abundant areas. We estimated the OH formation from the decomposition of CIs using a global atmospheric chemistry and transport model, STOCHEM-CRI (model description can be found in our previous publications[41-46] and found that in the terrestrial rainforest and boreal forest regions, up to 13% of OH radicals were formed via CI unimolecular decomposition (Figure 2). Thus, the amount of OH radicals produced from CI reactions in these areas can have a significant impact on the oxidizing capacity in the troposphere.
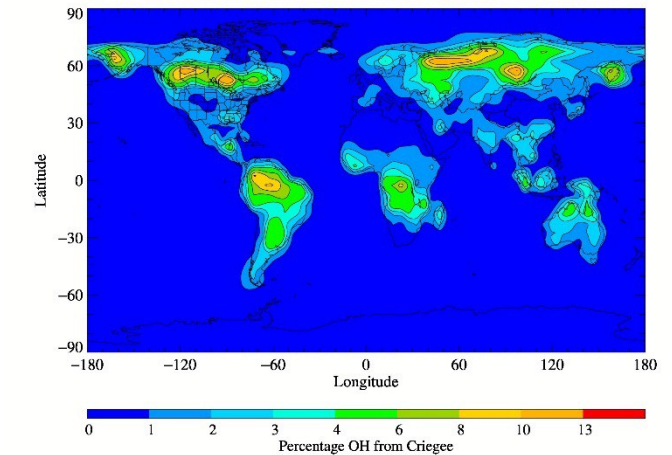

Figure 2. Estimation of the annual average percentage of OH formed from the CIs, simulated by the STOCHEM-CRI model.

ARTICLE

<div style="text-align:right">Journal Name</div>

Bimolecular reactions of Criegee Intermediates

Only a fraction of CI* (termed as sCIs) formed survive to undergo bimolecular reaction. These occur when either the initial CI* does not have sufficient energy to undergo unimolecular reaction or isomerisation, or the CI* are stabilised by collisions with a bath gas, M, (*e.g.* N_2 in the atmosphere).[11-12,47] sCIs can react with a variety of secondary compounds, 'Criegee scavengers', including: NO_x, SO_2, CO, water, water dimer, alcohols, aldehydes and carboxylic acids. However, in the atmosphere it is likely that only water, SO_2 and NO_x are of any appreciable concentration to act as sCI sinks. Historically, research has focused on the reaction of sCIs with water and it was assumed that HCOOH production was the major reaction pathway.[48] However, recent findings[21,23,24,25,31,34,49] have shown that rate constants for reaction with NO_2, SO_2 and carboxylic acids are significantly higher than previously thought. The direct measurements (through photolytic generation of Criegee intermediates using diiodoalkanes), indirect determinations (via ozonolysis measurements), and computational calculations give a wide range of the rate coefficient values for the bimolecular reactions (see Tables 2-6). Gaining a quantifiable understanding of the products and their distributions from these bimolecular reactions are important as they may have significant impacts on the troposphere.[42,50,51]

Table 2: Rate coefficient for the reaction of sCIs with water

Species	Rate coefficient (cm³ s⁻¹)		Temperature (K)	References
	Experimental	Theoretical		
CH_2OO		2.4×10^{-16}	298	Long et al.[19]
		3.7×10^{-16}	298	Lin et al.[52]
		3.1×10^{-15}	298	Anglada et al.[53]
		5.9×10^{-17}	298	Anglada et al.[54]
		8.2×10^{-18}	298	Ryzhkov and Ariya[55]
	$< 4 \times 10^{-15}$ ξ		298	Welz et al.[56]
	$(2.5 \pm 1.0) \times 10^{-17}$ ʸ,ᶠ		297	Ouyang et al.[25]
	$< 9 \times 10^{-17}$ ʸ,ᶠ		295	Stone et al.[57]
	$(1.3 \pm 0.4) \times 10^{-15}$ ʸ		298-303	Newland et al.[27]
	$<1.5 \times 10^{-15}$ ξ		298	Chao et al.[58]
	$(3.2 \pm 1.2) \times 10^{-16}$ ʸ		297 ± 1	Berndt et al.[20]
	$(2.4 \pm 1.6) \times 10^{-16}$ ξ		293	Sheps et al.[50]
syn-CH_3CHOO		5.7×10^{-20}	298	Long et al.[19]
		2.0×10^{-19}	298	Lin et al.[52]
		2.1×10^{-18}	298	Anglada et al.[53]
		4.2×10^{-20}	298	Anglada et al.[54]
		1.2×10^{-20}	298	Ryzhkov and Ariya[55]
	$<4 \times 10^{-15}$ ξ		298	Taatjes et al.[31]
	$<2 \times 10^{-16}$ ξ		298	Sheps et al.[59]
anti-CH_3CHOO		6.3×10^{-15}	298	Long et al.[19]
		3.4×10^{-14}	298	Lin et al.[52]
		1.7×10^{-13}	298	Anglada et al.[53]
		2.5×10^{-15}	298	Anglada et al.[54]
		6.7×10^{-16}	298	Ryzhkov and Ariya[55]
	$(2.3 \pm 2.1) \times 10^{-14}$		297-302	Newland et al.[29]
	$(1.0 \pm 0.4) \times 10^{-14}$ ξ		298	Taatjes et al.[31]
	$(2.4 \pm 0.4) \times 10^{-14}$ ξ		293	Sheps et al.[59]
	$(1.31 \pm 0.26) \times 10^{-14}$ ξ		298	Lin et al.[60]
$(CH_3)_2COO$		3.8×10^{-17}	298	Anglada et al.[53]
		7.5×10^{-19}	298	Anglada et al.[54]
		2.9×10^{-19}	298	Ryzhkov and Ariya[55]
	$(2.1 \pm 0.6) \times 10^{-15}$ ʸ		298-303	Newland et al.[29]
	$<1.5 \times 10^{-16}$ ξ		298	Huang et al.[61]

Note: ξThe values are from direct monitoring of the sCI decay, ʸThe values are from indirect sCI measurements. ᶠthe values from the experiments could not distinguish between the reaction with the water monomer or the dimer reaction.

Table 3: Rate coefficient for the reaction of sCIs with water dimer

$(H_2O)_2$	Rate coefficient (cm³ s⁻¹)		Temperature (K)	References
	Experimental	Theoretical		
CH_2OO		5.4×10^{-12}	298	Lin et al.[52]
		$(1.2-1.4) \times 10^{-12}$	298	Ryzhkov and Ariya[55]
	$(7.5 \pm 0.4) \times 10^{-12}$ ʸ		300	Liu et al.[62]
	$(6.5 \pm 0.8) \times 10^{-12}$ ξ		298	Chao et al.[58]
	$(7.4 \pm 0.6) \times 10^{-12}$ ξ		298	Smith et al.[63]
	$(4.0 \pm 1.2) \times 10^{-12}$ ξ		294	Lewis et al.[64]
	$(8.2 \pm 0.8) \times 10^{-12}$ ʸ		298 ± 2	Yajima et al.[65]
	$(6.6 \pm 0.7) \times 10^{-12}$ ξ		293	Sheps et al.[50]
syn-CH_3CHOO		2.6×10^{-14}	298	Lin et al.[52]
		$(1.0-1.2) \times 10^{-15}$	298	Ryzhkov and Ariya[55]
anti-CH_3CHOO		1.6×10^{-11}	298	Lin et al.[52]
		$(1.0-2.8) \times 10^{-12}$	298	Ryzhkov and Ariya[55]
	$(4.4 \pm 0.3) \times 10^{-11}$ ξ		298	Lin et al.[60]
$(CH_3)_2COO$		$(6.5-10.2) \times 10^{-17}$	298	Ryzhkov and Ariya[55]
	$<1.3 \times 10^{-13}$ ξ		298	Huang et al.[61]

Note: ξThe values are from direct monitoring of the sCI decay, ʸThe values are from indirect sCI measurements.

Table 4: Rate coefficient for the reaction of sCIs with NO_2

NO_2	Rate coefficient (cm³ s⁻¹)		Temperature (K)	References
	Experimental	Theoretical		
CH_2OO	$(7 +3/-2) \times 10^{-12}$ ξ		298	Welz et al.[56]
	$(1.5 \pm 0.5) \times 10^{-12}$ ʸ		295	Stone et al.[57]
		4.4×10^{-12}	298	Vereeken and Nguyen[66]
CH_3CHOO (*syn and anti*)	$(2.0 \pm 1.0) \times 10^{-12}$ ξ		298	Taatjes et al.[31]
	$(1.7 \pm 0.3) \times 10^{-12}$ ξ		298	Caravan et al.[67]
$(CH_3)_2COO$	$\leq 5 \times 10^{-12}$ ξ		298	Chhantyal-Pun et al.[34]

Note: ξThe values are from direct monitoring of the sCI decay, ʸThe values are from indirect sCI measurements.

Table 5: Rate coefficient for the reaction of sCIs with SO_2

SO_2	Rate coefficient ($cm^3 s^{-1}$)		Temperature (K)	References
	Experimental	Theoretical		
CH_2OO		4.0×10^{-10}	298	Kurtén et al.[68]
		$(3.68 \pm 0.02) \times 10^{-11}$	298	Kuwata et al.[69]
	$(3.9 \pm 0.7) \times 10^{-11\xi}$		298	Welz et al.[56]
	$(3.80 \pm 0.04) \times 10^{-11\xi}$		293	Chhantyal-Pun et al.[21]
	$(3.42 \pm 0.42) \times 10^{-11\Upsilon}$		295	Stone et al.[57]
	$(4.1 \pm 0.3) \times 10^{-11\xi}$		295	Sheps[24]
	$(3.53 \pm 0.29) \times 10^{-11\Upsilon}$		295	Liu et al.[23]
	$(3.3 \pm 0.9) \times 10^{-11\Upsilon}$		295 ± 2	Berndt et al.[70]
syn-CH_3CHOO	$(2.4 \pm 0.3) \times 10^{-11\xi}$		298	Taatjes et al.[31]
	$(2.9 \pm 0.3) \times 10^{-11\xi}$		293	Sheps et al.[59]
anti-CH_3CHOO	$(6.7 \pm 1.0) \times 10^{-11\xi}$		298	Taatjes et al.[31]
	$(22.0 \pm 2.0) \times 10^{-11\xi}$		293	Sheps et al.[59]
syn- and anti-CH_3CHOO	$(1.4 \pm 0.4) \times 10^{-13\Upsilon}$		293 ± 0.5	Berndt et al.[32]
$(CH_3)_2COO$		4.0×10^{-10}	298	Kurtén et al.[68]
	$(7.3 \pm 0.5) \times 10^{-11\xi}$		298	Chhantyal-Pun et al.[34]
	$(13.2 \pm 1.3) \times 10^{-11\xi}$		298	Huang et al.[61]
	$(7.7 \pm 1.4) \times 10^{-13\Upsilon}$		293 ± 0.5	Berndt et al[32]
β-pinene (C9)OO	$4.0 \times 10^{-11\Upsilon}$		298 ± 0.5	Ahrens et al.[71]

Note: $^{\xi}$The values are from direct monitoring of the sCI decay, $^{\Upsilon}$The values are from indirect sCI measurements.

Table 6: Rate coefficients for the reaction of sCIs with other species

Reaction	Rate coefficient ($cm^3 s^{-1}$)		Temperature (K)	References
	Experimental	Theoretical		
$CH_2OO + CH_3CHO$	$1.0 \times 10^{-12\Upsilon}$		298	Fenske et al.[33]
$CH_2OO + CH_3CHO$	$(9.4 \pm 0.7) \times 10^{-13\xi}$		293	Taatjes et al.[72]
$CH_2OO + CH_3CHO$	$(1.48 \pm 0.04) \times 10^{-12\Upsilon}$		295	Stone et al.[57]
$CH_2OO + CH_3CHO$	$(3.0 \pm 0.6) \times 10^{-13\xi}$		298	Elsamra et al.[73]
$CH_2OO + HCOOH$	$(1.1 \pm 0.7) \times 10^{-10\xi}$		298	Welz et al.[49]
$CH_2OO + HCOOH$	$(1.14 \pm 0.07) \times 10^{-10\xi}$		294	Chhantyal-Pun et al.[74]
syn-$CH_3CHOO + HCOOH$	$(2.5 \pm 0.3) \times 10^{-10\xi}$		298	Welz et al.[49]
anti-$CH_3CHOO + HCOOH$	$(5.0 \pm 3.0) \times 10^{-10\xi}$		298	Welz et al.[49]
$(CH_3)_2COO + HCOOH$	$(3.0 \pm 0.2) \times 10^{-10\xi}$		294	Chhantyal-Pun et al.[74]
$CH_2OO + CH_3COOH$	$(1.3 \pm 0.1) \times 10^{-10\xi}$		298	Welz et al.[49]
$CH_2OO + CH_3COOH$	$(1.47 \pm 0.07) \times 10^{-10\xi}$		294	Chhantyal-Pun et al.[74]
$CH_2OO + CH_3COOH$	$(1.25 \pm 0.3) \times 10^{-10\xi}$		295	Berndt et al.[70]
syn-$CH_3CHOO + CH_3COOH$	$(1.7 \pm 0.5) \times 10^{-10\xi}$		298	Welz et al.[49]
anti-$CH_3CHOO + CH_3COOH$	$(2.5 \pm 0.6) \times 10^{-10\xi}$		298	Welz et al.[49]
$(CH_3)_2COO + CH_3COOH$	$(3.3 \pm 0.2) \times 10^{-10\xi}$		294	Chhantyal-Pun et al.[74]
$CH_2OO + CF_3COOH$	$(3.4 \pm 0.3) \times 10^{-10\xi}$		294	Chhantyal-Pun et al.[75]
$CH_2OO + CClF_2COOH$	$(3.34 \pm 0.16) \times 10^{-10\xi}$		294	Chhantyal-Pun et al.[74]
$CH_2OO + CF_3CF_2COOH$	$(4.48 \pm 0.23) \times 10^{-10\xi}$		294	Chhantyal-Pun et al.[74]
$CH_2OO + Pyruvic acid$	$(0.2 \pm 0.02) \times 10^{-10\xi}$		294	Chhantyal-Pun et al.[74]
$(CH_3)_2COO + CF_3COOH$	$(3.4 \pm 0.3) \times 10^{-10\xi}$		294	Chhantyal-Pun et al.[75]
$(CH_3)_2COO + CClF_2COOH$	$(3.9 \pm 0.2) \times 10^{-10\xi}$		294	Chhantyal-Pun et al.[74]
$(CH_3)_2COO + CF_3CF_2COOH$	$(4.4 \pm 0.2) \times 10^{-10\xi}$		294	Chhantyal-Pun et al.[74]
$(CH_3)_2COO + Pyruvic acid$	$(0.9 \pm 0.1) \times 10^{-10\xi}$		294	Chhantyal-Pun et al.[74]
$CH_2OO + NO$	$< 6.0 \times 10^{-14\xi}$		298	Welz et al.[56]
$CH_2OO + NO$	$< 2.0 \times 10^{-13\Upsilon}$		295	Stone et al.[57]
$CH_2OO + CO$		2.0×10^{-21}	298	Vereecken et al.[76]
syn-$CH_3CHOO + CO$		7.0×10^{-21}	298	Vereecken et al.[76]
anti-$CH_3CHOO + CO$		8.0×10^{-20}	298	Vereecken et al.[76]
$(CH_3)_2COO + CO$		3.0×10^{-20}	298	Vereecken et al.[76]
$CH_2OO + CH_3COCH_3$	$(2.3 \pm 0.3) \times 10^{-13\xi}$		293	Taatjes et al.[72]
$CH_2OO + CH_3COCH_3$	$(1.2 \pm 0.2) \times 10^{-12\xi}$			Elsamra et al.[73]
$CH_2OO + O_3$		4.0×10^{-13}	298	Vereecken et al.[76]
syn-$CH_3CHOO + O_3$		3.0×10^{-14}	298	Vereecken et al.[76]
anti-$CH_3CHOO + O_3$		3.0×10^{-12}	298	Vereecken et al.[76]
$(CH_3)_2COO + O_3$		8.0×10^{-14}	298	Vereecken et al.[76]
$CH_2OO + HOOH$		3.0×10^{-13}	298	Vereecken et al.[76]
$CH_2OO + CH_3OOH$		6.0×10^{-12}	298	Vereecken et al.[76]
$(CH_3)_2COO + CH_3OOH$		8.0×10^{-13}	298	Vereecken et al.[76]
$CH_2OO + ethene$	$7 \times 10^{-16\xi}$		298	Buras et al.[77]
$CH_2OO + propene$	$18 \times 10^{-16\xi}$		298	Buras et al.[77]
$CH_2OO + isobutene$	$14 \times 10^{-16\xi}$		298	Buras et al.[77]
$CH_2OO + 1-butene$	$15 \times 10^{-16\xi}$		298	Buras et al.[77]
$CH_2OO + 2-butene$	$7 \times 10^{-16\xi}$		298	Buras et al.[77]
$CH_2OO + isoprene$	$(1.5 \pm 0.1) \times 10^{-15\xi}$		295	Decker et al.[78]
$CH_2OO + isoprene$	$(23 \pm 2) \times 10^{-15\xi}$		536	Decker et al.[78]
$CH_2OO + CH_2OO$	$7.4 \times 10^{-11\xi}$		293	Chhantyal-Pun et al.[21]
$CH_2OO + CH_2OO$	$8.0 \pm 4.0 \times 10^{-11\xi}$		295	Ting et al.[79]
$CH_2OO + CH_2OO$	$2.4 \times 10^{-10\xi}$		298	Su et al.[80]
$CH_2OO + CH_2OO$	$6.0 \times 10^{-11\xi}$		297	Buras et al.[77]
$CH_2OO + CH_2OO$	$2.2 \times 10^{-10\xi}$		343	Buras et al.[22]
$CH_2OO + H_2S$	$1.7 \pm 0.2 \times 10^{-13\xi}$		298	Smith et al.[81]
$CH_2OO + HNO_3$	$5.4 \times 10^{-10\xi}$		295	Foreman et al.[82]
$CH_2OO + HNO_3$		5.1×10^{-10}	295	Raghunath et al.[83]
$CH_2OO + HCl$	$4.6 \times 10^{-11\xi}$		295	Foreman et al.[82]
$CH_3(CH_2)_{11}CHOO + HCOOH$	$1.1 \times 10^{-10\Re}$		296 ± 3	Tobias and Ziemann[84]
$CH_3(CH_2)_{11}CHOO + C_6H_{13}COOH$	$2.8 \times 10^{-10\Upsilon}$		296 ± 3	Tobias and Ziemann[84]
$CH_3(CH_2)_{11}CHOO + HCHO$	$4.4 \times 10^{-11\Upsilon}$		296 ± 3	Tobias and Ziemann[84]
$CH_3(CH_2)_{11}CHOO + CH_3CH(OH)CH_3$	$8.3 \times 10^{-13\Upsilon}$		296 ± 3	Tobias and Ziemann[84]
$CH_3(CH_2)_{11}CHOO + CH_3OH$	$3.6 \times 10^{-13\Upsilon}$		296 ± 3	Tobias and Ziemann[84]
$CH_2OO + CH_3OH$	$3.7 \pm 1.4 \times 10^{-21} T^2 exp(1710 \pm 103/T)^{\xi}$			McGillen et al.[51]
$CH_2OO + C_2H_5OH$	$4.2 \pm 2.2 \times 10^{-21} T^2 exp(1717 \pm 145/T)^{\xi}$			McGillen et al.[51]
$(CH_3)_2COO + CH_3OH$	$6.1 \times 10^{-33} T^{3.87} exp(5852/T) + 5.8 \times 10^{-16} T^{2.92} exp(-3741/T)^{\xi}$			McGillen et al.[51]
$CH_2OO + CF_3C(O)CF_3$	$(3.0 \pm 0.3) \times 10^{-11\xi}$		293	Taatjes et al.[72]

Note: $^{\xi}$The values are from direct monitoring of the sCI decay, $^{\Upsilon}$The values are from indirect sCI measurements, $^{\Re}$we assume the rate coefficient of $CH_3(CH_2)_{11}CHOO + HCOOH$ as 1.1×10^{-10} $cm^3 s^{-1}$ (for CH_2OO literature) and estimate the rate coefficients of the reaction of $CH_3(CH_2)_{11}CHOO$ with $C_6H_{13}COOH$, HCHO, $CH_3CH(OH)CH_3$ and CH_3OH using the relative rate constants table from Tobias and Ziemann.[84]

The high concentration of water vapour in the lower troposphere (1.3×10^{17} to 8.3×10^{17} molecule cm^{-3})[61] makes it likely that the reaction of water with sCIs will be a dominant chemical sink. The energy barrier of the

sCI + H$_2$O reaction is reduced dramatically when interacting with a water dimer, as opposed to a monomer. Even though these dimers make up a small percentage (<1%) of water vapour, the reduced activation energy significantly increases the rate of the reaction.[52,55] Using the tropospheric water concentration estimated by Huang et al.[61], the tropospheric water dimer concentrations at 298 K are calculated to be in the range of 3.5×10^{13} to 1.4×10^{15} molecule cm^{-3}. The median rate coefficients for reaction with water and water dimer extracted from the reported values in Tables 2 and 3 are 3.2×10^{-16} and 5.4×10^{-12} cm^3 s^{-1} leading to loss rates at the surface of 40-270 s^{-1} and 190-7780 s^{-1} by water and water dimer, respectively. One of the main products of the reaction, sCI + water or water dimer is found to be hydroxymethyl hydroperoxide (HMHP).[50,85,86] The global atmospheric chemistry and transport model study estimated the levels of HMHP in the range of 10-200 ppt (Figure 3) with the highest peak found in terrestrial rain-forest regions.[50] However, HMHP itself can undergo decomposition to formic acid contributing to the acidity of precipitation.[87] It is known that HMHP has various toxic effects on plant cells and enzymes.[88-89] sCI formed from large functionalized or cyclic alkenes can react with water to form lower vapour pressure products (e.g. production of pinic acid from β-pinene suggested by Docherty and Ziemann[9] that are thought to be important species acting as Cloud Condensation Nuclei (CCN).
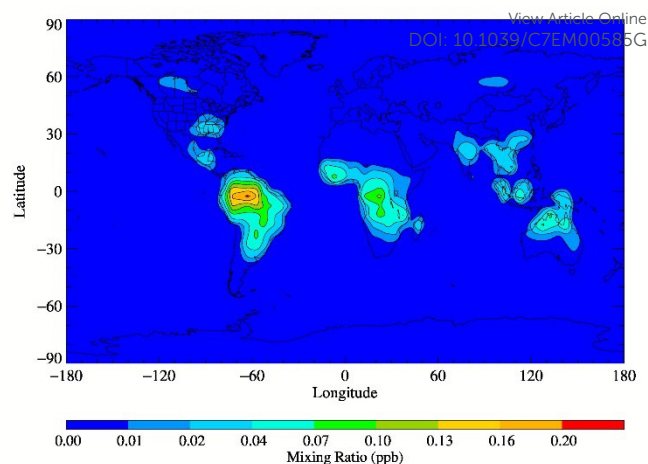
Figure 3. The estimated annual average surface HMHP produced from the sCI + water reaction simulated by the STOCHEM-CRI model (Adapted from Sheps et al.[50]).

A theoretical study[90] showed that, for CH$_2$OO and *anti*-CH$_3$CHOO, reaction with water and water dimer dominated the loss processes, even in a relatively low humidity environment such as Mexico City. Literature has shown that the rate coefficients for the reaction of sCI + water have a large dependence on the conformation of the sCI being considered, *anti*-sCIs are thought to react up to 5 orders of magnitude faster than *syn*-sCIs (see Table 2). Despite the slow reaction of *syn*-sCIs, they can go on to provide a source of OH radicals.[54] Alkene ozonolysis favours *syn*-formation and therefore these reactions can provide an essential source of atmospheric OH, and recent work[53,91] confirms this OH production pathway. For *anti*-CH$_3$CHOO, the median rate coefficient for reaction with water is 1.31×10^{-14} cm^3 s^{-1} leading to loss rate coefficients near Earth's surface of between $(1.7-10.8) \times 10^3$ s^{-1}, which greatly exceeds all estimates of the rate coefficient for unimolecular loss. For *syn*-CH$_3$CHOO the median rate coefficient for reaction with water is 2.0×10^{-19} cm^3 s^{-1} leading to loss rates at the surface between

Journal Name

ARTICLE

approximately 2.6×10^{-2} s^{-1} and 1.7×10^{-1} s^{-1} which is far smaller than estimates of the rate coefficients for unimolecular loss. For $(CH_3)_2COO$, the median rate coefficient for reaction with water is 3.8×10^{-17} cm^3 s^{-1} leading to loss rates at the surface between 10-30 s^{-1} which is similar to the rate coefficients for unimolecular loss, making both loss processes comparable. Therefore, for the few sCIs where data have been collected for both reactions, reaction with either the water monomer or dimer seems to be a dominant loss process. However, a much larger dataset, with larger sCIs, is needed to establish a more general prediction.

Although reactions with the water monomer and dimer may dominate removal of sCI, and thus other reaction pathways are of marginal importance in determining atmospheric sCI concentration, sCI can be substantial contributors to formation or removal of other species, particularly if sCI reactions can compete with reactions of OH. The oxidation of NO *via* sCIs to NO_2 is slow (6.0×10^{-14} cm^3 s^{-1}), which, along with the low tropospheric concentrations relative to water vapour, mean that this pathway is rarely considered to be of major importance.[90] This is supported in the work by Welz et al.[56] that shows even with [NO] = 5 x 10^{15} cm^{-3} no increase in the decay rate of the CH_2OO was observable. However, the oxidation of NO_2 *via* sCIs was found to be much faster than the reaction of NO + sCI (Table 4). Experiments have struggled to accurately ascertain information about the oxidation products of the reaction. Indirect kinetic measurements[25,92] suggested NO_3 formation from sCI+NO_2 under ambient atmospheric boundary layer conditions. However, Caravan et al.[67] demonstrated the formation of a Criegee-NO_2 adduct and found limited evidence for the NO_3 production channel (upper limit of 30%) in their direct measurement technique. The adduct formation as a competitor of NO_3 production makes the reaction of sCI + NO_2 a small contribution on NO_3 concentration, unless the adduct in turn generates NO_3 on longer kinetic timescales or through subsequent reactions.[67]

Oxidation of SO_2 by sCIs was believed to be of little tropospheric importance until relatively recently. Measurement of sCI oxidation of SO_2 can be difficult because the OH radicals resulting from CI decomposition can also compete. However, recently the direct kinetic measurement studies[21,23,31,34,56,57] showed that reaction rate constants for these reactions are up to 4 orders of magnitude larger than previously thought[33] and an order of magnitude larger than those reported for NO_2 for all sCIs studied (Table 5). The global atmospheric chemistry and transport model STOCHEM-CRI has been integrated showing that the oxidation of SO_2 by sCI is more significant (by up to 100%) in the terrestrial rain-forests and high latitude boreal forests compared with its oxidation by OH (Figure 4). The values are comparable with the study[93] who predicted up to 75% gas phase formation of H_2SO_4 from sCI +SO_2 relative to OH +SO_2 in the equatorial region. However, the modelling study of Sarwar et al.[94] showed that the oxidation of SO_2 by sCI has little impact on H_2SO_4 formation but decreasing the rate coefficient of the reaction of sCI with H_2O in the model can enhance the H_2SO_4 formation. The model has a limited number of alkenes producing limited sCIs, the loss processes detailed in Table 2-3 may play different roles for more complex sCIs. Thus, the main challenges facing accurate model predictions of steady state sCI

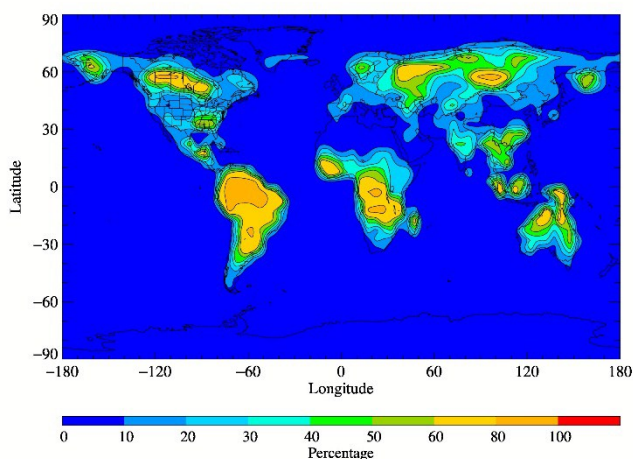and its impact on the troposphere is the many decades of uncertainty associated with the rate coefficients for water vapour.

Figure 4. The estimated percent contribution of the gas phase oxidation process of SO_2+sCI compared with the gas phase oxidation process of SO_2 +OH simulated by the STOCHEM-CRI model.

The SO_3 formed in these reactions[31,56,71] reacts with water vapour on very fast time-scales to form H_2SO_4.[32,95-97] Mauldin et al.[98] inferred the presence of sCI by investigating H_2SO_4 produced from the reaction, sCI+SO_2, this formation path had significance to reduce the discrepancy between measured and model H_2SO_4. Further study has shown that the oxidation of SO_2 by sCIs can rival the OH oxidation pathway in heavily polluted urban environments,[42] accounting for as much as 33-46% of H_2SO_4 production at ground level.[99]

Recent direct kinetic studies of the reaction of Criegee intermediates with organic acids have identified rate coefficients that are substantially higher,[73-75,100] than previous estimates based on theoretical calculations and/or end-product analysis (see Table 6), high enough that these reactions can potentially have significant impacts on the loss of sCI. The first order rate coefficient

ratio of the reactions sCI + acids is found to be one order magnitude higher relative to the reaction sCI + SO_2. It has been noted[30,101-103] that because of the very fast reaction of organic acids with sCI, they can be used to trap sCI in laboratory and field experiments. Recently, Chhantyal-Pun et al.[74] reported structure-specific rate coefficients for the reactions of various Criegee intermediates with different organic acids. Chhantyal-Pun et al.[75] also found that these reactions show relatively small temperature dependence over the temperature range found in lower troposphere. Incorporating these reactions of Criegee intermediates with organic acids (e.g. CH_3COOH, CF_3COOH) in the STOCHEM-CRI model[75,104] shows that loss of acids by sCI exceeds 60% of their total loss in South America, South Africa, Australia and parts of south East Asia resulting in large reductions of the life-time and burden of organic acids in these regions (Figure 5).
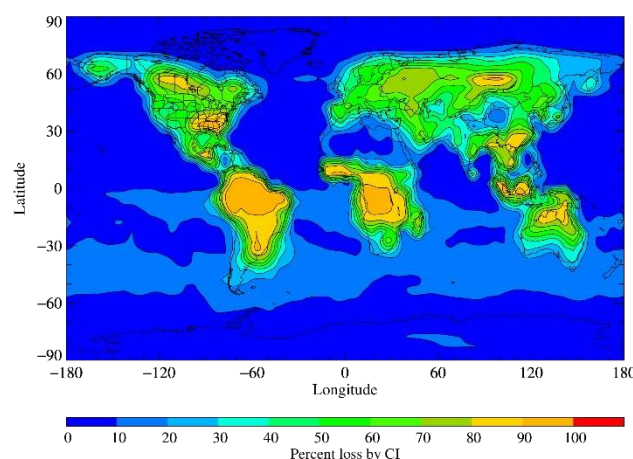

Figure 5. The estimated annual average CF_3COOH loss contribution by sCI simulated by the STOCHEM-CRI model (Adapted from Chhantyal-Pun et al.[75])

The rate coefficients for reactions of sCI with methanol and ethanol (Table 6) are ~ 1000 times smaller than

those for carboxylic acid reactions. In terms of loss of methanol and ethanol, the reactions with sCI are of minor importance, but they may be significant in the formation of gas-phase species e.g. α-alkoxyalkyl hydroperoxides (AAAH).[51] The STOCHEM-CRI model study suggests that up to 20 ppt of AAAH may be formed in terrestrial regions (Figure 6) where there are large emissions of alcohols and the precursors to sCIs. The formation of larger, more functionalized organic hydroperoxides derived from the reactions of more complicated sCIs, alcohols, or the secondary oxidation of primary AAAHs may be significant in terms of the formation of secondary organic aerosol (SOA) in the troposphere.[51]
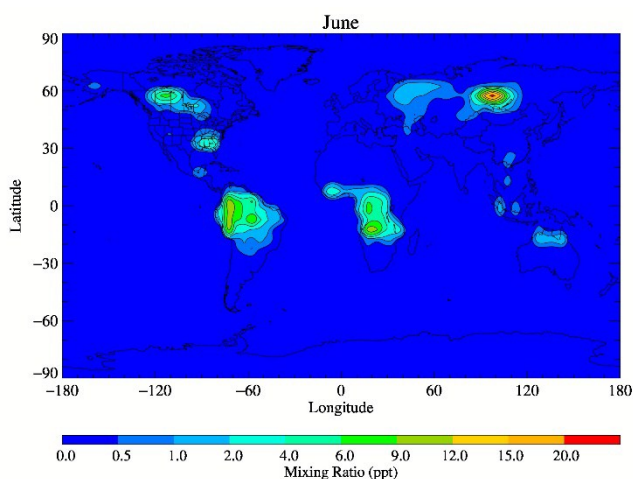
Figure 6. The estimated α-alkoxyalkyl hydroperoxide (AAAH) level from the reaction of sCI with methanol for the month of June, simulated by STOCHEM-CRI (Adapted from McGillen et al.[51]).

Estimation of regional and global sCI

sCIs are difficult to measure in the atmosphere due to their low steady state concentration, which is controlled by the slow rate of formation by ozonolysis and fast rate of destruction by various reactions (bimolecular or unimolecular). However, because the trace gases (e.g. O_3, unsaturated VOCs) that contribute to formation of sCI have been measured (National Environmental Technology Centre (NETCEN) data archive, http://uk-air.defra.gov.uk), a reasonable estimate of sCI can be made using the steady state approximation.[105] The levels of VOCs are high in the urban atmosphere because of their emissions from transport and other combustion sources, and these VOCs can then take part in photochemical ozone production in the downwind urban plume.[106-107] The elevated concentrations of ozone and increased levels of VOCs (e.g. alkenes) can lead to the formation of substantial sCI in the urban environment. The ozonolysis reactions of available 9 alkenes in the NETCEN data set, and an additional 43 alkenes modelled using information given by the Air Quality Improvement Research Program (AQIRP), give estimates of sCI concentrations of UK environments (e.g. 660 ± 650 cm^{-3} for London Eltham, 1960 ± 2390 cm^{-3} for London Marylebone Road and 590 ± 440 cm^{-3} for Harwell). The estimated sCI concentrations have a diurnal cycle with peaks during the afternoon, yearly cycle with peaks in Spring and weekly cycle with peaks on Sunday (see Figure 7). The sCI levels are predicted to be larger in the day time due to higher levels of VOCs, O_3 and higher temperature throughout the day. Moreover, the increased levels of O_3 along with higher temperature in spring months lead to an overall increase in sCI production in Spring. The variation of sCI between weekdays and weekend is not significant, although slightly higher levels are expected in the weekend because the lower traffic (i.e., low NO_x emissions) increases the VOC/NO_x ratio resulting in higher O_3 production. Using the estimated levels of urban sCI, the oxidation rate of SO_2 + sCI (37.6 Gg/yr) in urban areas is

ARTICLE

Journal Name

non-negligible compared with the most conventional oxidation rate of SO_2 + OH (0.64 Tg/yr) in urban areas.[105]

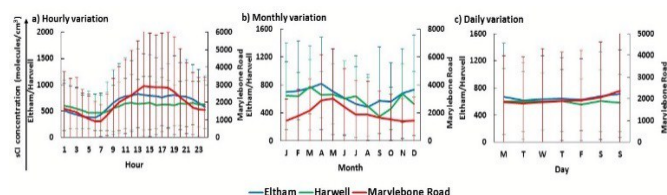Thus, these sCI reactions can alter the oxidizing capacity of the urban troposphere.

Figure 7. The hourly, monthly, and daily estimated sCI concentrations in the two urban sites and one rural site of UK (Adapted from Khan et al.[105]). The error bars represents ± 1 SD of the whole data series.

In the 3-D chemistry and transport model STOCHEM-CRI study, the Criegee field was generated using ozonolysis reactions of six alkenes (ethene, propene, *trans*-but-2-ene, isoprene, α-pinene and β-pinene) and their losses by water, water dimer and unimolecular decomposition. Based on the availability of experimental measurements and quantum calculations of the loss processes of different sCIs,[51] the Criegee field was created where the levels of sCI range from near zero up to levels approaching 6.0×10^5 cm^{-3}, with the highest levels predicted to be over regions of high biogenic emissions of reactive (unsaturated) hydrocarbons, e.g. the Amazon rain forest (see Figure 8a). A similar spatial distribution of sCI was shown by Vereecken et al.[93] with the peak sCI concentrations below 1.0×10^5 cm^{-3}. The Criegee chemistry used in STOCHEM-CRI is different from that of Vereecken et al.[93] (e.g. Vereecken et al. assigned rapid 1,5-ring closure for the isoprene-derived Criegee intermediates, MVKOO and MACROO during unimolecular decomposition) which can explain the higher sCI concentration estimation in our study. The

zonal plot from STOCHEM-CRI study shows that sCI levels estimated are highest (up to 7.0×10^4 cm^{-3}) in the tropics and fall dramatically with altitude (Figure 8b). The ozone levels are higher in the upper troposphere, but the alkene levels decrease with altitude because of their short lifetimes (typically days to hours). In addition, the decreased rate coefficients of the ozonolysis reactions because of the decreasing temperature further from the surface reduce the formation of sCI in the upper troposphere.
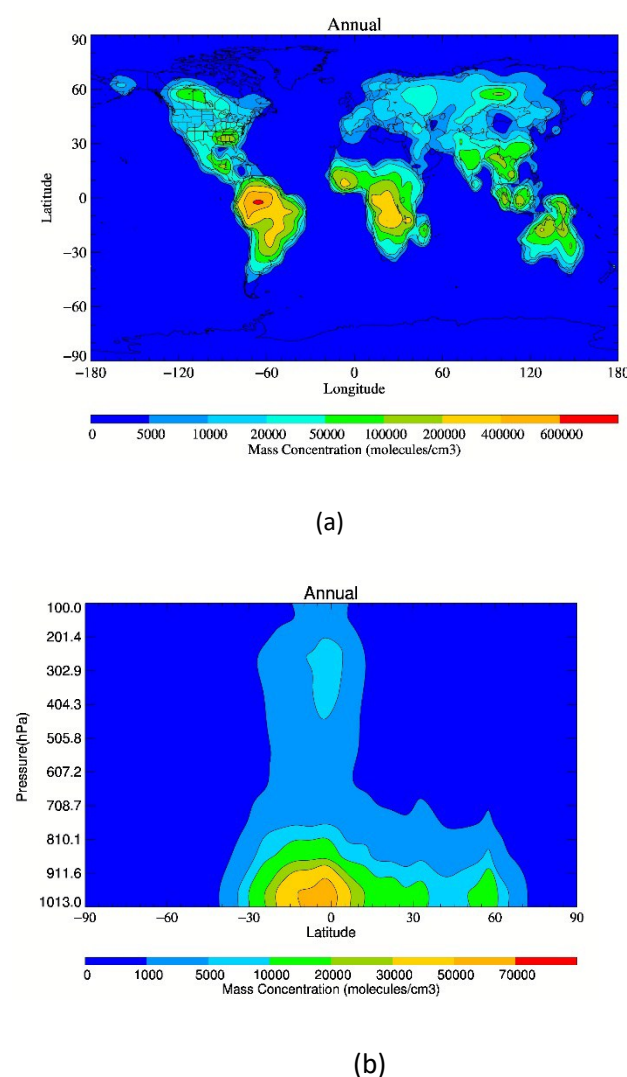

(a)

(b)

Figure 8. An estimate of annual average (a) surface levels (b) zonal levels of sCI derived using the global model, STOCHEM-CRI.

A variety of theoretical and field studies have also estimated levels of sCI using available measurements of alkenes and ozone. Vereecken et al.[90] estimated isoprene and monoterpene derived sCIs to be 1.2×10^4 cm^{-3} and 7.1×10^2 cm^{-3}, respectively at the tropical forest of Surinam using the steady state approximation. An indirect measurement, where the oxidation of SO_2 to H_2SO_4 in the presence of an OH scavenger is used to quantify the oxidant, gave sCI concentrations of ~5.0×10^4 cm^{-3} (with an order of magnitude uncertainty) for the boreal forest and rural environments of Finland and Germany.[108] However, the wall loss of sCI was not considered in their study which gives their estimate as a lower limit. Kim et al.[109] estimated peak sCI levels of ~5.5×10^4 cm^{-3} at ~5 pm downwind of the Dallas-Fort Worth, Texas conurbation, which are very similar to the study[99] who predicted sCI levels up to ~5×10^4 cm^{-3} in Hyytiälä, Finland, and Hohenpeissenberg, Germany. Bonn et al.[110] found sCI levels in the range of 2×10^4 cm^{-3} to 4×10^5 cm^{-3} during the day over the period August to September in the Mt. Kleiner Feldberg region in central Germany. In all cases, the oxidation of SO_2 by sCI at these calculated levels form an additional amount of H_2SO_4 which brings models into better agreement with measurements. However, Berresheim et al.[111] potentially detected sCI in the atmosphere at Mace Head in Ireland, using a CIMS-HO (HO instrument using Chemical Ionisation Mass Spectrometry) and found that the oxidation of SO_2 by sCI at Mace Head, Ireland can increase the H_2SO_4 concentrations by only 5-30% which is very small with respect to the average factor of 4.7 required to match the observed H_2SO_4 concentration. Analysis of all reported estimated sCIs levels gives a reasonable amount of sCI ~ $(1-5) \times 10^4$ cm^{-3} over the terrestrial boundary layer. However, direct measurements of sCI would be required for quantifying the changes of the tropospheric oxidizing capacity due to sCIs; failing that, more complete *in situ* measurements of the available alkene concentration can be used to calculate the sCI levels in different environments.[42,105] Detection of sCI in the atmosphere may soon become possible by direct measurement techniques such as near-UV cavity ringdown spectroscopy,[21] UV-Vis spectroscopy,[58,64] IR spectroscopy,[112] Proton transfer reaction time of flight mass spectrometry (PTR-TOF-MS),[113-114] or chemical ionisation mass spectrometry (CIMS).[70,115] However, it should be noted that direct measurements will represent a significant analytical challenge as a result of the low concentration of sCIs that are predicted in the atmosphere.

Potential importance of sCI on the troposphere

sCIs are important in the oxidative capacity and aerosol formation in the troposphere, and the high reactivity of sCI towards many key trace gas species (e.g. water vapour, SO_2, NO_2 and carboxylic acids) implies a greater role of sCIs in atmospheric chemistry than thought a decade ago. If we consider the level of sCI in the terrestrial boundary layer of the order of 1×10^4 cm^{-3} and the level of OH is of 1×10^6 cm^{-3}, ~10-fold larger k_{sCI} than k_{OH} is sufficient for the loss rate via reaction with sCI to compete with the loss by reaction with OH. The ratio of loss rates (Table 7) shows that some of the species (e.g. HNO_3, HCOOH, CH_3COOH, CF_3COOH, CF_3COCF_3, and pyruvic acid) where k_{sCI} is more than 100-

fold higher than k_{OH} resulting in the dominance of removal by sCI over OH. Thus, sCI makes a significant contribution to the oxidising capacity in the terrestrial boundary layer by reducing the estimated lifetime of these species and may lead to products that are condensable.[49]

For species such as HCl and SO_2, loss via reaction with OH and sCI are found to be comparable (Table 6). However, in the presence of higher sCI production, e.g., because of increased alkenes levels and increased temperature, oxidation of SO_2 by sCI can be of greater significance. Both field studies[98-100,108,116] and modelling studies[42,117-119] suggest that sCI could make a significant contribution (10-70%) to SO_2 oxidation (i.e., H_2SO_4 formation), but the extent of that contribution varies from study to study because of the different environmental conditions. The formation of H_2SO_4 from sCIs is atmospherically important because it can act as a CCN through the formation of secondary organic aerosol (SOA)[120] and can also acidify rain. The conversion of SO_2 into H_2SO_4 has been the focus of many research works, and understanding how H_2SO_4 influences cloud and SOA formation is of vital importance when modelling the direct and indirect effect of sCI.[121]

Table 7: Relative oxidation rates of some selected species by OH and sCI considering the concentrations of OH and sCI are 1×10^6 and 1×10^4 cm^{-3} respectively. Note: only CH_2OO is considered in the calculation.

Species	Rate coefficient of the reaction species + OH, k_{OH} (cm^3 s^{-1})	Rate coefficient of the reaction species +sCI, k_{sCI} (cm^3 s^{-1})	$k_{sCI}[sCI]/k_{OH}[OH]$
HNO_3	1.5×10^{-13} (Atkinson et al.[122])	5.4×10^{-10} (Foreman et al.[82])	**36**
HCOOH	4.5×10^{-13} (Atkinson et al.[123])	1.1×10^{-10} (Welz et al.[49])	**2.5**
CH_3COOH	8.0×10^{-13} (Atkinson et al.[123])	1.3×10^{-10} (Welz et al.[49])	**1.6**
CF_3COOH	1.4×10^{-13} (Atkinson et al.[123])	3.4×10^{-10} (Chhantyal-Pun et al.[75])	**24.3**
HCl	8.0×10^{-13} (Atkinson et al.[123])	4.6×10^{-11} (Foreman et al.[82])	0.6
NO_2	4.1×10^{-11} (Atkinson et al.[122])	7.0×10^{-12} (Welz et al.[56])	0.002
SO_2	1.3×10^{-12} (Atkinson et al.[122])	3.8×10^{-11} (Chhantyal-Pun et al.[21])	0.3
CH_3CHO	1.6×10^{-11} (Atkinson et al.[123])	1.5×10^{-12} (Stone et al.[57])	0.001
CH_3COCH_3	2.2×10^{-13} (Atkinson et al.[123])	1.2×10^{-12} (Elsamra et al.[72])	0.06
CH_3OH	9.0×10^{-13} (Atkinson et al.[123])	1.0×10^{-13} (McGillen et al.[51])	0.001
C_2H_5OH	3.2×10^{-12} (Atkinson et al.[123])	1.2×10^{-13} (McGillen et al.[51])	0.0004

For some other species (e.g. CH_3OH, C_2H_5OH, CH_3CHO), k_{OH} is higher than k_{sCI} resulting in the dominance of removal by OH over sCI. However, this type of species, especially with a C=O, C-O-O-H, C-O-H and C-O-O moieties, can react with sCI to form adducts.[35] Synchrotron-based photoionization mass spectrometry measurements demonstrate that the adduct products formed from the reactions of sCI and organic acids, such adducts will have low vapour pressures and high O:C ratios which may lead to condensation of organic species and secondary organic aerosol (SOA) formation.[49,74] Therefore, even though these reactions only represent a small fraction of the loss compared with the loss by OH, it may be important because of its contribution to SOA formation, with associated impacts on air quality and climate.

There are laboratory[124-125] and chamber studies[126] that showed that reactions between sCI and RO_2 (peroxy

radicals) and organic hydroperoxides (ROOH) can form addition products (Figure 9).
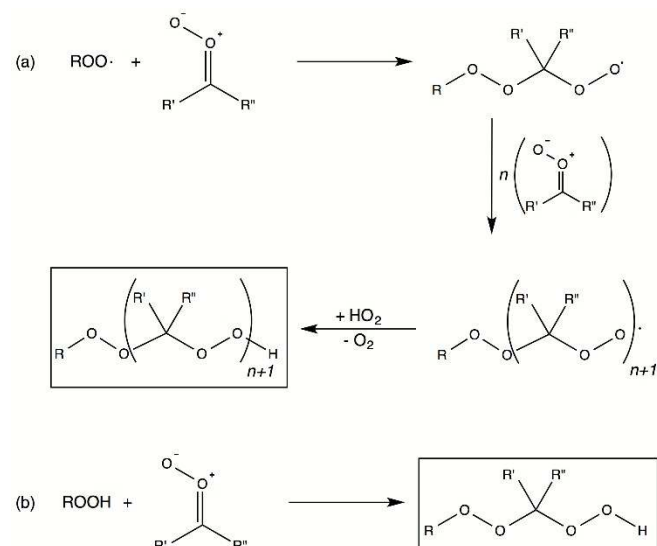

Figure 9. Mechanism for the sequential addition of sCI to (a) peroxy radical and (b) an organic hydroperoxide

Global model studies suggest that the highest concentrations of RO_2 up to 50 pptv[44] and ROOH up to 8 ppbv[45] are found in Amazon rainforest region, where the concentration of sCI is also found to be greatest. So, the oxidations of RO_2 and ROOH by sCI may be prominent in these regions, and if the products of these reactions are the adducts shown in Figure 9, these reactions may be significant for SOA formation. However, the large uncertainties of both rate coefficients and the product branching make quantification of these reaction channels difficult. Nevertheless, global model estimates of the distribution of [sCI]*[RO_2] and [sCI]*[ROOH] shows that elevated [sCI]*[RO_2] and [sCI]*[ROOH] exist over the tropical regions (Figure 10 and 11). In summary, the oxidation of VOCs by sCIs is likely to yield highly oxygenated species which can lead to nucleation and the formation of SOA and the extent to which these

reactions are affecting the regional and global climate is still to be determined.
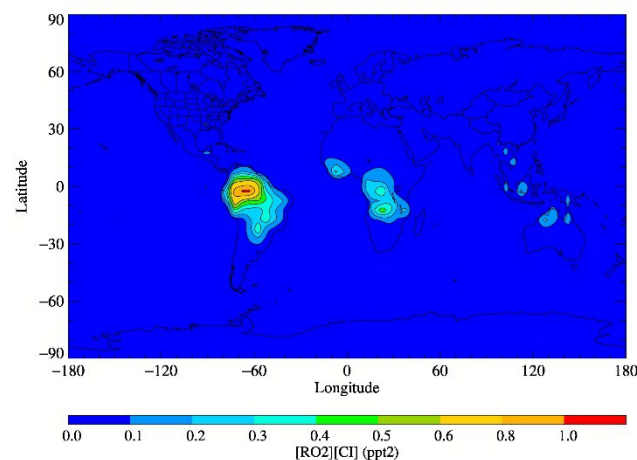

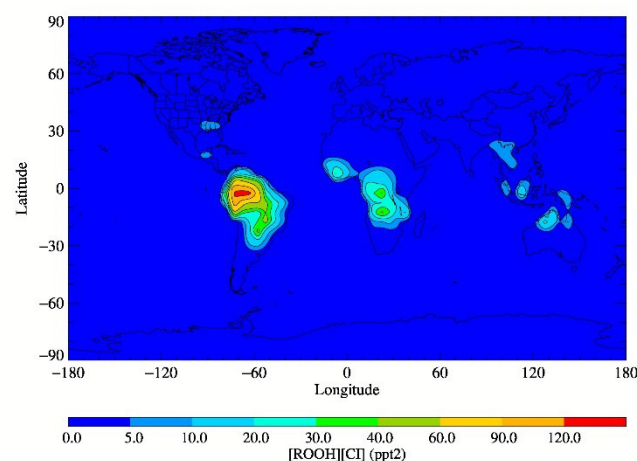Figure 10. Annual average surface estimate of the product [sCIs][RO_2] using fields derived from the STOCHEM-CRI global model.

Figure 11. Annual average surface estimate of the expression [sCIs][ROOH] using fields derived from the STOCHEM-CRI global model.

Conclusions

The oxidation of alkenes via reaction with ozone act as a major sink for alkenes in the troposphere and has been established to yield Criegee intermediates. The unimolecular decomposition of these species is thought to be contributed to the formation of OH which is significant in the tropospheric oxidation cycle during nighttime and winter months. A variety of model-

measurement studies estimated the surface levels of the Criegee intermediates in the order of 10^4 cm^{-3} to 10^5 cm^{-3}, the peak level was found over regions of high biogenic emissions e.g. the Amazon rain forest. The direct detection of Criegee intermediate and measurements of the reaction kinetics of Criegee with several important tropospheric species, NO_2, SO_2, water, water dimer, carboxylic acid, alcohols, aldehydes, ketones suggest that Criegee reactions are important in terms of the product information and their tropospheric distribution. The potential role of these intermediates in atmospheric chemistry is significant, altering our thinking about the oxidising capacity of the Earth's atmosphere and the rate of formation of SOA. Currently, the steady state estimation of sCIs and its impact on the troposphere is a complex task because of the underlying uncertainties of the unimolecular and bimolecular rate coefficients of larger and more complicated sCIs especially biologically important species (e.g. isoprene and terpenes) derived sCIs. Future research should be focused on the direct measurement of the unimolecular and bimolecular rate co-efficient of the loss processes of sCIs with longer alkyl chain in order to predict the global burden of sCI and also on the experimental determination of sCIs which will be beneficial to validate the model results.

Conflicts of interest

There are no conflicts to declare.

Acknowledgements

Notes and references

[1] R. Criegee and G. Wenner. Die Ozonisierung des 9,10-Oktalins. *Liebigs. Ann. Chem.*, 1949, **564**, 9-15.

[2] R. Criegee. Mechanism of ozonolysis. *Angew. Chem. Inter. Ed.*, 1975, **14**, 745–752.

[3] O. Horie and G. K. Moortgat. Decomposition pathways of the excited Criegee intermediates in the ozonolysis of simple alkenes. *Atmos. Environ.*, 1991, **25**, 1881–1896.

[4] D. E. Shallcross, K. E., Leather, A. Bacak, P. Xiao, E. P. F. Lee, M. Ng, D. K. W. Mok, J. M. Dyke, R. Hossaini, M. P. Chipperfield, M. A. H. Khan and C. J. Percival. Reaction between CH_3O_2 and BrO radicals: A new source of upper Troposphere Lower Stratosphere hydroxyl radicals. *J. Phys. Chem. A*, 2015, **119**, 4618–4632.

[5] E. Assaf, L. Sheps, L. Whalley, D. Heard, A. Tomas, C. Schoemaecker and C. Fittschen. The reaction between CH3O2 and OH radicals: product yields and atmospheric implications. *Environ. Sci. Technol.*, 2017, **51**, 2170-2177.

[6] T. P. W. Jungkamp, A. Kukui and R. N. Schindler. Determination of rate constants and product branching ratios for the reactions of CH_3O_2 and CH_3O with Cl atoms at room temperature. *Ber. Bunsenges. Phys. Chem.*, 1995, **99**, 1057–1066.

[7] M. S. Alam, A. R. Rickard, M. Camredon, K. P. Wyche, T. Carr, K. E. Hornsby, P. S. Monks and W. J. Bloss. Radical product yields from the ozonolysis of short chain alkenes under atmospheric boundary layer conditions. *J. Phys. Chem. A.,* 2013, **117**, 12468–12483.

[8] A. S. Hasson, G. Orzechowska, S. E. Paulson. Production of stabilized Criegee intermediates and peroxides in the gas phase ozonolysis of alkenes. 1. Ethene, trans-2-butene, and 2,3-dimethyl-2-butene. *J. Geophys. Res.*, 2001, **106**, 34131-34142.

[9] K. S. Docherty and P. J. Ziemann. Effects of stabilized Criegee intermediate and OH radical scavengers on aerosol formation from reactions of β-pinene with O_3. *Aerosol Sci. Technol.*, 2003, **37**, 877-891.

[10] N. M. Donahue, J. H. Kroll, J. G. Anderson and K. L. Demerjian. Direct observation of OH production from the ozonolysis of olefins. *Geophys. Res. Lett.*, 1998, **25**, 59–62.

[11] J. H. Kroll, J. S. Clarke, N. M. Donahue, J. G. Anderson and K. L. Demerjian. Mechanism of HO_x formation in the gas-phase ozone-alkene reaction. 1. Direct, pressure dependent measurement of prompt OH yields. *J. Phys. Chem. A*, 2001, **105**, 1554-1560.

[12] J. H. Kroll, S. R. Sahay and J. G. Anderson. Mechanism of HO_x formation in the gas-phase ozone-alkene reaction. 2. Prompt versus thermal dissociation of carbonyl oxides to form OH. *J. Phys. Chem. A*, 2001, **105**, 4446–4457.

[13] J. H. Kroll, N. M. Donahue, V. J. Cee, K. L. Demerjian and J. G. Anderson. Gas-phase ozonolysis of alkenes: Formation of OH from anti carbonyl oxides. *J. Am. Chem. Soc.*, 2002, **124**, 8518–8519.

[14] M. Siese, K. H. Becker, K. J. Brockmann, H. Geiger, A. Hofzumahaus, F. Holland, M. Milhelcic, and K. Wirtz. Direct measurement of OH radicals from ozonolysis of selected alkenes: a EUPHORE simulation chamber study. *Environ. Sci. Technol.*, 2001, **35**, 4660–4667.

[15] A. M. Green, V. P. Barber, Y. Fang, S. J. Klippenstein, and M. I. Lester. Selective deuteration illuminates the importance of tunneling in the unimolecular decay of Criegee intermediates to hydroxyl radical products, *Proc. Nat. Acad. Sci.*, 2017, **114**, 12372-12377.

[16] R. Gutbrod, R. N. Schindler, E. Kraka and D. Cremer. Formation of OH radicals in the gas phase ozonolysis of alkenes, the unexpected role of carbonyl oxides. *Chem. Phys. Lett.*, 1996, **252**, 221-229.

[17] M. Olzmann, E. Kraka, D. Cremer, R. Gutbrod and S. Andersson. Energetics, kinetics, and product distributions of the reactions of ozone with ethene and 2,3-dimethyl-2-butene. *J. Phys. Chem. A*, 1997, **101**, 9421–9429.

[18] T. L. Nguyen, M. C. McCarthy and J. F. Stanton. Relatively selective production of the simplest Criegee intermediate in a CH_4/O_2 electric discharge: Kinetic analysis of a plausible mechanism. *J. Phys. Chem. A*, 2015, **119**, 7197–7204.

[19] B. Long, J. L. Bao and D. G. Truhlar. Atmospheric chemistry of Criegee intermediates: Unimolecular reactions and reactions with water. *J. Am. Chem. Soc.*, 2016, **138**, 14409–14422.

[20] T. Berndt, R. Kaethner, J. Voigtlander, F. Stratmann, M. Pfeifle, P. Reichle, M. Sipila, M. Kulmala and M. Olzmann. Kinetics of the unimolecular reaction of CH_2OO and the bimolecular reactions with the water monomer, acetaldehyde and acetone under atmospheric conditions. *Phys. Chem. Chem. Phys.*, 2015, **17**, 19862–19873.

[21] R. Chhantyal-Pun, A. Davey, D. E. Shallcross, C. J. Percival and A. J. Orr-Ewing. A kinetic study of the CH_2OO Criegee intermediate self-reaction, reaction with SO_2 and unimolecular reaction using cavity ring-down spectroscopy. *Phys. Chem. Chem. Phys.*, 2015, **17**, 3617–3626.

[22] Z. J. Buras, R. M. I. Elsamra and W. H. Green. Direct determination of the simplest Criegee intermediate (CH_2OO) self-reaction rate. *J. Phys. Chem. Letts.*, 2014, **5**, 2224–2228.

[23] Y. Liu, K. D. Bayes and S. P. Sander. Measuring rate constants for reactions of the simplest Criegee intermediate (CH_2OO) by monitoring the OH radical. *J. Phys. Chem. A*, 2014, **118**, 741–747.

[24] L. Sheps. Absolute ultraviolet absorption spectrum of a Criegee intermediate CH_2OO. *J. Phys. Chem. Letts.*, 2013, **4**, 4201–4205.

[25] B. Ouyang, M. W. McLeod, R. L. Jones and W. J. Bloss. NO_3 radical production from the reaction between the Criegee intermediate CH_2OO and NO_2. *Phys. Chem. Chem. Phys.*, 2013, **15**, 17070–17075.

[26] K. T. Kuwata, M. R. Hermes, M. J. Carlson and C. K. Zogg. Computational studies of the isomerization and hydration reactions of acetaldehyde oxide and methyl vinyl carbonyl oxide. *J. Phys. Chem. A*, 2010, **114**, 9192–9204.

[27] Y. Fang, F. Liu, V. P. Barber, S. J. Klippenstein, A. B. McCoy and M. I. Lester. Communication: Real time observation of unimolecular decay of Criegee intermediates to OH radical products. *J. Chem. Phys.*, 2016, **144**, 061102.

[28] J. T. Herron, R. I. Martinez and R. E. Huie. Kinetics and energetics of the Criegee intermediate in the gas phase. I. The Criegee intermediate in ozone-alkene reactions. *Int. J. Chem. Kinet.*, 1982, **14**, 201–224.

[29] M. J. Newland, A. R. Rickard, L. Vereecken, A. Muňoz, M. Ródenas and W. J. Bloss. Atmospheric isoprene ozonolysis: impacts of stabilized Criegee intermediate reactions with SO_2, H_2O and dimethyl sulphide. *Atmos. Chem. Phys.*, 2015, **15**, 9521–9536.

[30] A. Novelli, L. Vereecken, J. Lelieveld and H. Harder. Direct observation of OH formation from stabilised Criegee intermediates. *Phys. Chem. Chem. Phys.*, 2014, **16**, 19941–19951.

[31] C. A. Taatjes, O. Welz, A. J. Eskola, J. D. Savee, A. M. Scheer, D. E. Shallcross, B. Rotavera, E. P. F. Lee, J. M. Dyke, D. K. W. Mok, D. L. Osborn and C. J. Percival. Direct measurements of conformer-dependent reactivity of the Criegee intermediate CH_3CHOO. *Science*, 2013, **340**, 177–180.

[32] T. Berndt, T. Jokinen, R. L. Mauldin, III, T. Petäjä, H. Herrmann, H. Junninen, P. Paasonen, D. R. Worsnop and M. Sipilä. Gas-phase ozonolysis of selected olefins: The yield of stabilized Criegee intermediate and the reactivity toward SO2. *J. Phys. Chem. Letts.*, 2012, **3**, 2892–2896.

[33] J. D. Fenske, A. S. Hasson, A. W. Ho and S. E. Paulson. Measurement of absolute unimolecular and bimolecular rate constants for CH_3CHOO generated by the trans-2-butene reaction with ozone in the gas phase. *J. Phys. Chem. A*, 2000, **104**, 9921–9932.

[34] R. Chhantyal-Pun, O. Welz, J. D. Savee, A. J. Eskola, E. P. F. Lee, L. Blacker, H. R. Hill, M. Ashcroft, M. A. H. Khan, G. C. Lloyd-Jones, L. Evans, B. Rotavera, H. Huang, D. L. Osborn, D. K. W. Mok, J. M. Dyke, D. E. Shallcross, C. J. Percival, A. J. Orr-Ewing and C. A. Taatjes. Direct measurements of unimolecular and bimolecular reaction kinetics of the Criegee intermediate $(CH_3)_2COO$. *J. Phys. Chem. A*, 2017, **121**, 4–15.

[35] M. C. Smith, W. Chao, K. Takahashi, K. A. Boering and J. Jr-M. Lin. Unimolecular decomposition rate of the Criegee intermediate $(CH_3)_2COO$ measured directly with UV absorption spectroscopy. *J. Phys. Chem. A*, 2016, **120**, 4789–4798.

[36] M. J. Newland, A. R. Rickard, T. Sherwen, M. J. Evans, L. Vereecken, A. Muñoz, M. Ródenas and W. J. Bloss. The atmospheric impacts of monoterpene ozonolysis on global stabilised Criegee intermediate budgets and SO_2 oxidation: experiment, theory and modelling. *Atmos. Chem. Phys. Discuss.*, 2017, doi.org/10.5194/acp-2017-1095.

[37] R. M. Harrison, J. Yin, R. M. Tilling, X. Cai, P. W. Seakins, J. R. Hopkins, D. L. Lansley, A. C. Lewis, M. C. Hunter, D. E. Heard, L. J. Carpenter, D. J. Creasy, J. D. Lee, M. J. Pilling, N. Carslaw, K. M. Emmerson, A. Redington, R. G. Derwent, D. Ryall, G. Mills and S. A. Penkett. Measurement and modelling of air pollution: Overview of the PUMA consortium project. *Sci. Total Env.*, 2006, **360**, 5–25.

[38] C. A. Taatjes, D. E. Shallcross and C. J. Percival. Research frontiers in the Chemistry of Criegee intermediates and tropospheric ozonolysis. *Phys. Chem. Chem. Phys.*, 2014, **16**, 1704–1718.

[39] Y. F. Elshorbany, J. Kleffmann, R. Kurtenbach, M. Rubio, E. Lissi, G. Villena, E. Gramsch, A. R. Rickard, M. J. Pilling, P. Wiesen. Summertime photochemical ozone formation in Santiago, Chile. *Atmos. Environ.*, 2009, **43**, 6398-6407.

[40] D. Johnson and G. Marston. The gas-phase ozonolysis of unsaturated volatile organic compounds in the troposphere. *Chem. Soc. Rev.*, 2008, **37**, 699–716.

[41] S. R. Utembe, M. C. Cooke, A. T. Archibald, M. E. Jenkin, R. G. Derwent, D. E. Shallcross. Using a reduced common representative intermediates (CRIv2-R5)mechanism to simulate tropospheric ozone in a 3-D Lagrangian chemistry transport model. *Atmos. Environ.*, 2010, **44**, 1609-1622.

[42] C. J. Percival, O. Welz, A. J. Eskola, J. D. Savee, D. L. Osborn, D. O. Topping, D. Lowe, S. R. Utembe, A. Bacak, G. McFiggans, M. C. Cooke, P. Xiao, A. T. Archibald, M. E. Jenkin, R. G. Derwent, D. W. K. Mok, E. P. F. Lee, J. M. Dyke, C. A. Taatjes and D. E. Shallcross. Regional and global impacts of Criegee intermediates on atmospheric aerosol nucleation rates. *Faraday Discuss.*, 2013, **165**, 45–73.

[43] M. A. H. Khan, M. C. Cooke, S. R. Utembe, P. Xiao, R. G. Derwent, M. E. Jenkin, A. T. Archibald, P. Maxwell, W. C. Morris, N. South, C. J. Percival and D. E. Shallcross. Reassessing the photochemical production of methanol from peroxy radical self and cross reactions using the STOCHEM-CRI global chemistry and transport model. *Atmos. Environ.*, 2014, **99**, 77-84.

[44] M. A. H. Khan, M. C. Cooke, S. R. Utembe, A. T. Archibald, R. G. Derwent, M. E. Jenkin, W. C. Morris, N. South, J. C. Hansen, J. S. Francisco, C. J. Percival and D. E. Shallcross. Global analysis of peroxy radicals and peroxy radical-water complexation using the STOCHEM-CRI global chemistry and transport model. *Atmos. Environ.*, 2015, **106**, 278–287.

[45] M. A. H. Khan, M. C. Cooke, S. R. Utembe, P. Xiao, W. C. Morris, R. G. Derwent, A. T. Archibald, M. E. Jenkin, C. J. Percival, D. E. Shallcross. The global budgets of organic hydroperoxides for present and pre-industrial scenarios. *Atmos. Environ.*, 2015, **110**, 65-74.

[46] M. A. H. Khan, M. C. Cooke, S. R. Utembe, W. C. Morris, A. T. Archibald, R. G. Derwent, M. E. Jenkin, A. J. Orr-Ewing, C. M. Higgins, C. J. Percival, K. E. Leather and D. E. Shallcross, Global modeling of the C1-C3 alkyl nitrates using STOCHEM-CRI. *Atmos. Environ.*, 2015, **123**, 256-267.

[47] G. T. Drozd and N. M. Donahue. Pressure dependence of stabilized Criegee intermediate formation from a sequence of alkenes. *J. Phys. Chem.*, 2011, **115**, 4381-4387.

[48] P Neeb, F. Sauer, O. Horie and G. K. Moortgat. Formation of hydroxymethyl hydroperoxide and formic acid in alkene ozonolysis in the presence of water vapour. *Atmos. Environ.*, 1997, **31**, 1417-1423 (1997).

[49] O. Welz, A. J. Eskola, L. Sheps, B. Rotavera, J. D. Savee, A. M. Scheer, D. L. Osborn, D. Lowe, A. M. Booth, P. Xiao, M. A. H. Khan, C. J. Percival, D. E. Shallcross and C. A. Taatjes. Rate

coefficients of C1 and C2 Criegee intermediate reactions with formic and acetic acid near the collision limit: Direct kinetic measurements and atmospheric implications. *Angew. Chem. Int. Ed.*, 2014, **53**, 4547–4550.

[50] L. Sheps, B. Rotavera, A. J. Eskola, D. L. Osborn, C. A. Taatjes, K. Au, D. E. Shallcross, M. A. H. Khan and C. J. Percival. The reaction of Criegee intermediate CH_2OO with water dimer: primary products and atmospheric impact. *Phys. Chem. Chem. Phys.*, 2017, **19**, 21970-21979.

[51] M. R. McGillen, B. F. E. Curchod, R. Chhantyal-Pun, J. M. Beames, N. Watson, M. A. H. Khan, L. McMahon, D. E. Shallcross, A. J. Orr-Ewing. Criegee intermediate-alcohol reactions, a potential source of functionalized hydroperoxides in the atmosphere. *ACS Earth Space Chem*., 2017, 1, 664-672.

[52] L. C. Lin, H. T. Chang, C. H. Chang, W. Chao, M. C. Smith, C. H. Chang, J. J. M. Lin and K. Takahashi. Competition between H_2O and $(H_2O)_2$ reactions with CH_2OO/CH_3CHOO. *Phys. Chem. Chem. Phys.*, 2016, **18**, 4557–4568.

[53] J. M. Anglada, J. González and M. Torrent-Sucarrat. Effects of the substituents on the reactivity of carbonyl oxides. A theoretical study on the reaction of substituted carbonyl oxides with water. *Phys. Chem. Chem. Phys.*, 2011, **13**, 13034–13045.

[54] J. M. Anglada, P. Aplincourt, J. M. Bofill and D. Cremer. Atmospheric formation of OH radicals and H_2O_2 from alkene ozonolysis under humid conditions. *Chemphyschem*, 2002, **2**, 215–221.

[55] A. B. Ryzhkov and P. A. Ariya. A theoretical study of the reactions of parent and substituted Criegee intermediates with water and the water dimer. *Phys. Chem. Chem. Phys.,* 2004, **6**, 5042–5050.

[56] O. Welz, J. D. Savee, D. L. Osborn, S. S. Vasu, C. J. Percival, D. E. Shallcross and C. A. Taatjes. Direct kinetic measurements of Criegee intermediate (CH_2OO) formed by reaction of CH_2I with O_2. *Science*, 2012, **335**, 204–207.

[57] D. Stone, M. Blitz, L. Daubney, N. U. M. Howes and P. Seakins. Kinetics of CH_2OO reactions with SO_2, NO_2, NO, H_2O and CH_3CHO as a function of pressure. *Phys. Chem. Chem. Phys.*, 2014, **16**, 1139–1149.

[58] W. Chao, J. –T. Hsieh, C. –H. Chang and J. J. –M. Lin. Direct kinetic measurement of the reaction of the simplest Criegee intermediate with water vapor. *Science*, 2015, **347**, 751–754.

[59] L. Sheps, A. M. Scully and K. Au. UV absorption probing of the conformer-dependent reactivity of a Criegee intermediate CH_3CHOO. *Phys. Chem. Chem. Phys.*, 2014, **16**, 26701–26706.

[60] L. C. Lin, W. Chao, C. H. Chang, K. Takahashi and J. J. M. Lin. Temperature dependence of the reaction of *anti*-CH_3CHOO with water vapor. *Phys. Chem. Chem. Phys.*, 2016, **18**, 28189–28197.

[61] H. –L. Huang, W. Chao, J. Jr–M. Lin. Kinetics of a Criegee intermediate that would survive high humidity and may oxidize atmospheric SO_2. *Proc. Natl. Acad. Sci.*, 2015, **112**, 10857–10862.

[62] Y. Liu, F. Liu, S. Liu, D. Dai, W. Dong and X. Yang. A kinetic study of the CH_2OO Criegee intermediate reaction with SO_2, $(H_2O)_2$, CH_2I_2 and I atoms using OH laser induced fluorescence. *Phys. Chem. Chem. Phys.*, 2017, **19**, 20786-20794.

[63] M. C. Smith, C. H. Chang, W. Chao, L. C. Lin, K. Takahashi, K. A. Boering and J. J. M. Lin. Strong negative temperature dependence of the simplest Criegee intermediate CH_2OO reaction with water dimer. *J. Phys. Chem. Letts.*, 2015, **6**, 2708–2713.

[64] T. R. Lewis, M. A. Blitz, D. E. Heard and P.W. Seakins. Direct evidence for a substantive reaction between the Criegee intermediate, CH_2OO, and the water vapour dimer. *Phys. Chem. Chem. Phys.*, 2015, **17**, 4859–4863.

[65] R. Yajima, Y. Sakamoto, S. Inomata and J. Hirokawa. Relative reactivity measurements of stabilized CH_2OO, produced by ethene ozonolysis, toward acetic acid and water vapour using chemical ionization mass spectrometry. *J. Phys. Chem. A*, 2017, **121**, 6640-6449.

[66] L. Vereecken and H. M. T. Nguyen. Theoretical study of the reaction of carbonyl oxide with nitrogen dioxide: CH_2OO + NO_2. *Inter. J. Chem. Kinet.*, 2017, **49**, 752-760.

[67] R. Caravan, M. A. H. Khan, B. Rotavera, E. Papajak, I. O. Antonov, M.-W. Chen, K. Au, W. Chao, D. L. Osborn, J. Jr-M. Lin, C. J. Percival, D. E. Shallcross and C. A. Taatjes. Products of Criegee intermediate reactions with NO_2: Experimental measurements and tropospheric implications. *Faraday Diss.*, 2017, **200**, 313-330.

[68] T. Kurtén, J. R. Lane, S. Jørgensen and H. G. Kjaergaard. A computational study of the oxidation of SO_2 to SO_3 by gas-phase organic oxidants. *J. Phys. Chem. A*, 2011, **115**, 8669–8681.

[69] K. T. Kuwata, E. J. Guinn, M. R. Hermes, J. A. Fernandez, J. M. Mathison and K. Huang. A computational re-examination of the Criegee intermediate-sulfur dioxide reaction. *J. Phys. Chem. A*, 2015, **119**, 10316–10335.

[70] T. Berndt, H. Herrmann and T. Kurten. Direct probing of Criegee intermediates from gas-phase ozonolysis using chemical ionization mass spectrometry. J. Am. Chem. Soc., 2017, **139**, 13387-13392.

[71] J. Ahrens, P. T. M. Carlsson, N. Hertl, M. Olzmann, M. Pfeifle, J. L. Wolf and T. Zeuch. Infrared detection of Criegee

ARTICLE

Journal Name

intermediates formed during the ozonolysis of β-pinene and their reactivity towards sulfur dioxide. *Angew. Chem. Int. Ed.*, 2014, **53**, 715–719.

[72] C. A. Taatjes, O. Welz, A. J. Eskola, J. D. Savee, D. L. Osborn, E. P. F. Lee, J. M. Dyke, D. W. K. Mok, D. E. Shallcross and C. J. Percival. Direct measurement of Criegee intermediate (CH_2OO) reactions with acetone, acetaldehyde, and hexafluoroacetone. *Phys. Chem. Chem. Phys.*, 2012, **14**, 10391–10400.

[73] R. M. Elsamra, A. Jalan, Z. J. Buras, J. E. Middaugh and W. H. Green. Temperature and pressure-dependent kinetics of CH_2OO + CH_3COCH_3 and CH_2OO + CH_3CHO: Direct measurements and theoretical analysis. *Int. J. Chem. Kinet.*, 2016, **48**, 474-488.

[74] R. Chhantyal-Pun, B. Rotavera, M. R. McGillen, M. A. H. Khan, A. J. Eskola, R. L. Caravan, L. Blacker, D. P. Tew, D. L. Osborn, C. J. Percival, C. A. Taatjes, D. E. Shallcross and A. J. Orr-Ewing. Reactive removal of tropospheric carboxylic acids by Criegee Intermediate, 2018, (Unpublished data).

[75] R. Chhantyal-Pun, M. R. McGillen, J. M. Beames, M. A. H Khan, C. J. Percival, D. E. Shallcross, A. J. Orr-Ewing. Temperature-dependence of the rates of reaction of trifluoroacetic acid with Criegee intermediates. *Angew. Chem. Int. Ed. Engl.*, 2017, **56**, 9044–9047.

[76] L. Vereecken, A. R. Rickard, M. J. Newland and W. J. Bloss. Theoretical study of the reactions of Criegee intermediates with ozone, alkylhydroperoxides, and carbon monoxide. *Phys. Chem. Chem. Phys.*, 2015, **17**, 23847–23858.

[77] Z. J. Buras, R. M. I. Elsamra, A. Jalan, J. E. Middaugh, W. H. Green. Direct kinetic measurements of reactions between the simplest Criegee intermediate CH_2OO and alkenes. *J. Phys. Chem. A*, 2014, **118**, 1997–2006.

[78] Z. C. J. Decker, K Au, L. Vereecken and L. Sheps. Direct experimental probing and theoretical analysis of the reaction between the simplest Criegee intermediate CH_2OO and isoprene. *Phys. Chem. Chem. Phys.*, 2017, **19**, 8541-8551.

[79] W. L. Ting, C. H. Chang, Y. F. Lee, H. Matsui, Y. P. Lee and J. J. M. Lin. Detailed mechanism of the CH_2I + O_2 reaction: Yield and self-reaction of the simplest Criegee intermediate CH_2OO. *J. Chem. Phys.*, 2014, **141**, 104308.

[80] Y. -T. Su, H. Y. Lin, R. Putikam, H. Matsui, M. C. Lin and Y. P. Lee. Extremely rapid self-reaction of the simplest Criegee intermediate CH_2OO and its implications in atmospheric chemistry. *Nature Chem.*, 2014, **6**, 477–483.

[81] M. C. Smith, W. Chao, M. Kumar, J. S. Francisco, K. Takahashi and J. J. M. Lin. Temperature-dependent rate coefficients for the reaction of CH_2OO with hydrogen sulphide. *J. Phys. Chem. A*, 2017, **121**, 938–945.

[82] E. S. Foreman, K. M. Kapnas and C. Murray. Reactions between Criegee intermediates and the inorganic acids HCl and HNO_3: Kinetics and atmospheric implications. *Angew. Chem. Int. Ed.*, 2016, **55**, 10419–10422.

[83] P. Raghunath, Y. P. Lee and M. C. Lin. Computational chemical kinetics for the reaction of Criegee intermediate CH_2OO with HNO_3 and its catalytic conversion to OH and HCO. *J. Phys. Chem. A*, 2017, **121**, 3871-3878.

[84] H. J. Tobias and P. J. Ziemann. Kinetics of the gas-phase reactions of alcohols, aldehydes, carboxylic acids, and water with the C13 stabilized Criegee intermediate formed from ozonolysis of 1-Tetradecene. *J. Phys. Chem. A*, 2001, **105**, 6129–6135.

[85] T. B. Nguyen, G. S. Tyndall, J. D. Crounse, A. Teng, K. H. Bates, R. H. Schwantes, M. M. Coggon, L. Zhang, P. Feiner, D. O. Miller, K. Skog, J. C. Rivera-Rios, M. Dorris, K. F. Olson, A. Koss, R. J. Wild, S. Brown, A. H. Goldstein, J. de Gouw, W. H. Brune, F. N. Keutsch, J. H. Seinfeld and P. Wennberg. Atmospheric fates of Criegee intermediates in the ozonolysis of isoprene. *Phys. Chem. Chem. Phys.*, 2016, **18**, 10241-10254.

[86] M. Nakajima and Y. Endo. Observation of hydroxymethyl hydroperoxide in a reaction system containing CH2OO and water vapor through pure rotational spectroscopy. *J. Chem. Phys.*, 2015, **143**, 164307.

[87] D. B. Millet, M. Baasandorj, D. K. Farmer, J. A. Thornton, K. Baumann, P. Brophy, S. Chaliyakunnel, J. A. de Gouw, M. Graus, L. Hu, A. Koss, B. H. L. Lee, F. D. Lopez-Hilfiker, J. A. Neuman, F. Paulot, J. Peischl, I. B. Pollack, T. B. Ryerson, C. Warneke, B. J. Williams and J. Xu. A large and ubiquitous source of atmospheric formic acid. *Atmos. Chem. Phys.*, 2015, **15**, 6283-6304.

[88] S. Marklund. Biochim. Biophys. Acta, The actions of hydroxymethylhydroperoxide and bis(hydroxymethyl)peroxide on fumarate hydratase, lactate dehydrogenase, aspartate aminotransferase, glucose oxidase and acid phosphatase. 1972, 258, 9-16.

[89] S. Marklund. Mechanisms of the irreversible inactivation of horseradish peroxidase caused by hydroxymethylhydroperoxide, Biochem. Biophys., 1973, 154, 614-622.

[90] L. Vereecken, H. Harder and A. Novelli. The reaction of Criegee intermediates with NO, RO_2, and SO_2, and their fate in the atmosphere. *Phys. Chem. Chem. Phys.*, 2012, **14**, 14682–14695.

[91] L. Jiang, R. Lan, Y. -S. Xu, W. J-. Zhang, W. Yang. Reaction of stabilized Criegee intermediates from ozonolysis of limonene with water: ab initio and DFT study. *Int. J. Mole. Sci.*, 2013, **14**, 5784-5805.

ARTICLE

[92] A. Presto and N. Donahue. Ozonolysis fragment quenching by nitrate formation: The pressure dependence of prompt OH radical formation. *J. Phys. Chem. A*, 2004, **108**, 9096–9104.

[93] L. Vereecken, A. Novelli and D. Taraborrelli. Unimolecular decay strongly limits the atmospheric impact of Criegee intermediates. *Phys. Chem. Chem. Phys.*, 2017, **19**, 31599-31612.

[94] G. Sarwar, K. Fahey, R. Kwok, R. C. Gilliam, S. J. Roselle, R. Mathur, J. Xue, J. Yu and W. P. L. Carter. Potential impacts of two SO2 oxidation pathways on regional sulfate concentrations: Aqueous-phase oxidation by NO₂ and gas-phase oxidation by stabilized Criegee Intermediates. *Atmos. Environ.*, 2013, **68**, 186-197.

[95] R. A. Cox and S. A. Penkett. Oxidation of atmospheric SO₂ by products of ozone olefin reaction. *Nature*, 1972, **230**, 321-322.

[96] S. Hatakeyama and H. Akimoto. Reactions of Criegee intermediates in the gas-phase. *Res. Chem. Inter.*, 1994, **20**, 503–524.

[97] T. Berndt, J. Voigtlander, F. Stratmann, H. Junninen, R. L. Mauldin, M. Sipila, M. Kulmala and H. Herrmann. Competing atmospheric reactions of CH₂OO with SO₂ and water vapour. *Phys. Chem. Chem. Phys.*, 2014, **16**, 19130–19136.

[98] R. L. Mauldin III, T. Berndt, M. Sipila, P. Paasonen, T. Petaja, S. Kim, T. Kurten, F. Stratmann, V. M. Kerminen and M. Kulmala. A new atmospherically relevant oxidant of sulphur dioxide. *Nature*, 2012, **488**, 193–196.

[99] M. Boy, D. Mogensen, S. Smolander, L. Zhou, T. Nieminen, P. Paasonen, C. Plass-Dulmer, M. Sipila, T. Petaja, L. Mauldin, H. Berresheim and M. Kulmala. Oxidation of SO₂ by stabilized Criegee intermediate (sCI) radicals as a crucial source for atmospheric sulfuric acid concentrations. *Atmos. Chem. Phys.*, 2013, **13**, 3865–3879.

[100] M. Sipilä, T. Jokinen, T. Berndt, S. Richters, R. Makkonen, N. M. Donahue, R. L. Mauldin, T. Kurtén, P. Paasonen, N. Sarnela, M. Ehn, H. Junninen, M. P. Rissanen, J. Thornton, F. Stratmann, H. Herrmann, D. R. Worsnop, M. Kulmala, V. –M. Kerminen and T. Petäjä. Reactivity of stabilized Criegee intermediates (sCIs) from isoprene and monoterpene ozonolysis toward SO₂ and organic acids. *Atmos. Chem. Phys.*, 2014, **14**, 12143–12153.

[101] S. Wolff, A. Boddenberg, J. Thamm, W. V. Turner and S. Gab. Gas phase ozonolysis of ethene in the presence of carbonyl oxide scavengers. *Atmos. Environ.*, 1997, **31**, 2965-2969.

[102] P. Neeb, O. Horie and G. K. Moortgat. Gas phase ozonolysis of ethene in the presence of hydroxylic compounds. *Int. J. Chem. Kinet.*, 1996, **28**, 721-730.

[103] A. Sadezky, P. Chaimbault, A. Mellouki, A. Rompp, R. Winterhalter, G. K. Moortgat and G. Le Bras. Formation of secondary organic aerosol and oligomers from the ozonolysis of enol ethers. *Atmos. Chem. Phys.*, 2006, **6**, 5009-5024.

[104] M. A. H. Khan, K. Lyons, R. Chhantyal-Pun, M. R. McGillen, R. L. Caravan, C. A. Taatjes, A. J. Orr-Ewing, C. J. Percival, D. E. Shallcross. Investigating the tropospheric chemistry of acetic acid using the global 3-D chemistry transport model, STOCHEM-CRI, Unpublished data, 2018.

[105] M. A. H. Khan, W. C. Morris, M. Galloway, B. M. A. Shallcross, C. J. Percival and D. E. Shallcross. An estimation of the levels of stabilized Criegee intermediates in the UK urban and rural atmosphere using the steady-state approximation and the potential effects of these intermediates on tropospheric oxidation cycles. *Int. J. Chem. Kinet.*, 2017, **49**, 611-621.

[106] S. Sillman, The relation between ozone, NOx and hydrocarbons in urban and polluted rural environments. *Atmos. Environ.*, 1999, **33**, 1821-1845.

[107] M. E. Jenkin and K. C. Clemitshaw. Ozone and other secondary photochemical pollutants: chemical processes governing their formation in the planetary boundary layer. *Atmos. Environ.*, 2000, **34**, 2499–2527.

[108] A Novelli, K. Hens, C. T. Ernest, M. Martinez, A. C. Nolscher, V. Sinha, P. Paasonen, T. Petaja, M. Sipila, T. Elste, C. Plass-Dulmer, G. J. Phillips, D. Kubistin, J. Williams, L. Vereecken, J. Lelieveld and H. Harder. Estimating the atmospheric concentration of Criegee intermediate and their possible interference in a FAGE-LIF instrument. *Atmos. Chem. Phys.*, 2017, **17**, 7807-7826.

[109] S. Kim, A. Guenther, B. Lefer, J. Flynn, R. Griffin, A. P. Rutter, L. W. Gong and B. K. Cevik. Potential role of stabilized Criegee radicals in sulfuric acid production in a high biogenic VOC environment. *Environ. Sci. Technol.*, 2015, **49**, 3383–3391.

[110] B. Bonn, E. Bourtsoukidis, T. S. Sun, H. Bingemer, L. Rondo, U. Javed, J. Li, R. Axinte, X. Li, T. Brauers, H. Sonderfeld, R. Koppmann, A. Sogachev, S. Jacobi and D. V. Spracklen. The link between atmospheric radicals and newly formed particles at a spruce forest site in Germany. *Atmos. Chem. Phys.*, 2014, **14**, 10823–10843.

[111] H. Berresheim, M. Adam, C. Monahan, C. O'Dowd, J. M. C. Plane, B. Bohn and F. Rohrer. Missing SO₂ oxidant in the coastal atmosphere?-observations from high-resolution

measurements of OH and atmospheric sulfur compounds. *Atmos. Chem. Phys.*, 2014, **14**, 12209–12223.

[112] Y. -T. Su, Y.-H. Huang, H. A. Witek, Y.-P. Lee. Infrared absorption spectrum of the simplest Criegee intermediate CH_2OO. *Science*, 2013, **340**, 174-176.

[113] C. Giorio, S. J. Campbell, M. Bruschi, A. T. Archibald, M. Kalberer. Detection and identification of Criegee intermediates from the ozonolysis of biogenic and anthropogenic VOCs: comparison between experimental measurements and theoretical calculations. *Faraday Discus.*, 2017, **200**, 559-578.

[114] M. Breitenlechner, A. Zaytsev, J. Kroll, A. Hansel and F. N. Keutsch. Unambiguous detection of speciated stabilized Criegee intermediates via gas phase derivatization followed by detection using mass spectrometry. *EGU General Assembly Conference Abstract*, 2017, **19**, 11603.

[115] M. Riva, S. H. Budisulistiorini, Z. F. Zhang, A. Gold, J. A. Thornton, B. J. Turpin and J. D. Surratt. Multiphase reactivity of gaseous hydroperoxide oligomers produced from isoprene ozonolysis in the presence of acidified aerosols. *Atmos. Environ.*, 2017, **152**, 314–322.

[116] T. Liu, X. Wang, Q. Hu, W. Deng, Y. Zhang, X. Ding, X. Fu, F. Bernard, Z. Zhang, S. Lu, Q. He, X. Bi, J. Chen, Y. Sun, J. Yu, P. Peng, G. Sheng, J. Fu. Formation of secondary aerosols from gasoline vehicle exhaust when mixing with SO_2. *Atmos. Chem. Phys.*, 2016, **16**, 675–689.

[117] J. Y. Li, Q. Ying, B. Yi and P. Yang. Role of stabilized Criegee intermediates in the formation of atmospheric sulfate in eastern United States. *Atmos. Environ.*, 2013, **79**, 442–447.

[118] G. Sarwar, H. Simon, K. Fahey, R. Mathur, W. S. Goliff and W. R. Stockwell. Impact of sulfur dioxide oxidation by stabilized Criegee intermediate on sulfate. *Atmos. Environ.*, 2014, **85**, 204–214.

[119] Q. Ying, I. V. Cureno, G. Chen, S. Ali, H. L. Zhang, M. Malloy, H. A. Bravo and R. Sosa. Impacts of stabilized Criegee intermediates, surface uptake processes and higher aromatic secondary organic aerosol yields on predicted PM2.5 concentrations in the Mexico City metropolitan zone. *Atmos. Environ.*, 2014, **94**, 438–447.

[120] M. Kulmala, U. Pirjola and J. M. Makela. Stable sulphate clusters as a source of new atmospheric particles. *Nature*, 2000, **404**, 66–69.

[121] V. Fiedler, M. D. Maso, M. Boy, H. Aufmhoff, J. Hoffmann, T. Schuck, W. Birmili, M. Hanke, J. Uecker, F. Arnold and M. Kulmala. The contribution of sulphuric acid to atmospheric particle formation and growth: a comparison

between boundary layers in Northern and Central Europe. *Atmos. Chem. Phys.*, 2005, **5**, 1773-1785.

[122] R. Atkinson, D. L. Baulch, R. A. Cox, J. N. Crowly, R. F. Hampson, R. G. Hynes, M. E. Jenkin, M. J. Rossi and J. Troe. Evaluated kinetic and photochemical data for atmospheric chemistry: Volume I-gas phase reactions of Ox, HOx, NOx and SOx species. *Atmos. Chem. Phys.*, 2004, **4**, 1461-1738.

[123] R. Atkinson, D. L. Baulch, R. A. Cox, R. F. Hampson, J. A. Kerr, M. J. Rossi and J. Troe. Evaluated kinetic, photochemical and heterogeneous data for atmospheric chemistry: Supplement V. IUPAC Subcommittee on gas kinetic data evaluation for atmospheric chemistry. *J. Phys. Chem. Ref. Data*, 1997, **26**, 521-1010.

[124] A. Sadezky, R. Winterhalter, B. Kanawati, A. Roempp, B. Spengler, A. Mellouki, G. Le Bras, P. Chaimbault and G. K. Moortgat. Oligomer formation during gas-phase ozonolysis of small alkenes and enol ethers: new evidence for the central role of the Criegee intermediate as oligomer chain unit. *Atmos. Chem. Phys.*, 2008, **8**, 2667–2699.

[125] Y. Sakamoto, S. Inomata and J. Hirokawa. Oligomerization reaction of the Criegee intermediate leads to secondary organic aerosol formation in ethylene ozonolysis. *J. Phys. Chem. A*, 2013, **117**, 12912-12921.

[126] Y. Zhao, L. M. Wingen, V. Perraud, J. Greaves and B. J. Finlayson-Pitts. Role of the reaction of stabilized Criegee intermediates with peroxy radicals in particle formation and growth in air. *Phys. Chem. Chem. Phys.*, 2015, **17**, 12500–12514 (2015).